

**Innovations Deserving
Exploratory Analysis Programs**

High-Speed Rail IDEA Program

**Crash Energy Absorption for High-Speed Rail Passenger
Seats Using Solid Ejection Material**

Final Report for High-Speed Rail IDEA Project 45

Prepared by:
Stephen E. Knotts
Paragrate

June 2007

TRANSPORTATION RESEARCH BOARD
OF THE NATIONAL ACADEMIES

INNOVATIONS DESERVING EXPLORATORY ANALYSIS (IDEA) PROGRAMS MANAGED BY THE TRANSPORTATION RESEARCH BOARD

This investigation was performed as part of the High-Speed Rail IDEA program supports innovative methods and technology in support of the Federal Railroad Administration's (FRA) next-generation high-speed rail technology development program.

The High-Speed Rail IDEA program is one of four IDEA programs managed by TRB. The other IDEA programs are listed below.

- NCHRP Highway IDEA focuses on advances in the design, construction, safety, and maintenance of highway systems, is part of the National Cooperative Highway Research Program.
- Transit IDEA focuses on development and testing of innovative concepts and methods for improving transit practice. The Transit IDEA Program is part of the Transit Cooperative Research Program, a cooperative effort of the Federal Transit Administration (FTA), the Transportation Research Board (TRB) and the Transit Development Corporation, a nonprofit educational and research organization of the American Public Transportation Association. The program is funded by the FTA and is managed by TRB.
- Safety IDEA focuses on innovative approaches to improving motor carrier, railroad, and highway safety. The program is supported by the Federal Motor Carrier Safety Administration and the FRA.

Management of the four IDEA programs is integrated to promote the development and testing of nontraditional and innovative concepts, methods, and technologies for surface transportation.

For information on the IDEA programs, contact the IDEA programs office by telephone (202-334-3310); by fax (202-334-3471); or on the Internet at <http://www.trb.org/idea>

IDEA Programs
Transportation Research Board
500 Fifth Street, NW
Washington, DC 20001

The project that is the subject of this contractor-authored report was a part of the Innovations Deserving Exploratory Analysis (IDEA) Programs, which are managed by the Transportation Research Board (TRB) with the approval of the Governing Board of the National Research Council. The members of the oversight committee that monitored the project and reviewed the report were chosen for their special competencies and with regard for appropriate balance. The views expressed in this report are those of the contractor who conducted the investigation documented in this report and do not necessarily reflect those of the Transportation Research Board, the National Research Council, or the sponsors of the IDEA Programs. This document has not been edited by TRB.

The Transportation Research Board of the National Academies, the National Research Council, and the organizations that sponsor the IDEA Programs do not endorse products or manufacturers. Trade or manufacturers' names appear herein solely because they are considered essential to the object of the investigation.

***Crash Energy Absorption for
High-Speed Rail Passenger Seats
Using Solid Ejection Material***

IDEA Program Final Report
For the Period June 2003 through June 2007
Contract Number HSR-45

Prepared for
The IDEA Program
Transportation Research Board
National Research Council

Stephen E. Knotts
Paragrate

June 2007

ACKNOWLEDGMENTS:

While this was a relatively small study effort, the ability to complete the needed test planning, hardware design, materials acquisition, test hardware fabrication and testing was the result of the actions and assistance of a small team.

Charles Taylor, the High Speed Rail-IDEA project manager – for his consideration and insight, to see the potential of a fundamentally unexploited crash shock technology, and for his guidance and support. And while at this stage of development it may appear that making seat shock modifications to an already spec approved seat design may not be advantageous; the study provided a great deal of useful proof testing, data and insight for this new crash energy absorption technology, which will surely aid in the launching of future application markets.

Kris Severson (Volpe) –Ms. Severson’s experience with past Volpe crash tests, along with her foresight in terms of test plan formation helped to reduce test failures in a number of areas. Suggestions, such as the need for preliminary impact barrier testing to assure the spec impact pulse was delivered; general seat setup with proper spacing; the need for replacement seats for each test due to the likelihood of damage, even with shock modifications; and the need for moment loading in the static tests of the SEM seat shocks; all of these suggestions proved to be extremely relevant in the two test efforts conducted at TTI. Undoubtedly fewer test runs would have been achieved if Ms. Severson’s suggestions had not been followed.

Dean Alberson (Texas Transportation Institute) – Mr. Alberson has been very helpful over the years in the testing and potential marketing of the SEM shock technology. Plus without his assistance in getting the TTI test facilities involved in this test effort, no crash testing would have been conducted within the budget constraints of this study. In the most recent test effort Mr. Alberson was even helping the Principal Investigator on test hardware prep on the weekend, to assure the first test run could be conducted that following Monday. Again his assistance over the years on development of the SEM technology is much appreciated, and Mr. Alberson’s help has been crucial to SEM shock technology’s progression.

Gerry Honeman (Stanfield, Co.) – Another group who also deserves acknowledgement and mention is the Stanfield Co., managed by Gerry Honemann. His company contributed its expertise in general metal fabrication, along with its supply and machining connections, to fabricate all of the test hardware that was used in the TTI/SEM test effort. Some of that hardware consisted of very large and very complex parts. The TTI test efforts in 2004 and 2005 would not have been achievable without Mr. Honemann’s support.

Craig Rehburg (Boeing) – Mr. Rehburg performed the FEM analysis for all of the major test hardware, to assure its operation in a series of impact tests. And because of that FEM analysis all of the major test hardware (e.g. Bogie, impact barrier) performed flawlessly.

Kam Yeung (Dennis) Chung, SPC 4/10 MTN HHC BDE, with a MS in Applied Mathematics – Mr. Chung’s early assistance in the motions formulas proved invaluable in the design, sizing and tailoring of the impact barrier’s performance.

ABSTRACT AND KEYWORDS:

This project assessed the potential of Solid Ejection Material (SEM) crash energy absorption technology for High-Speed Rail applications. A basic SEM model consists of an impact piston inside of a shock housing, and the end of the piston inside the housing is in contact with a ductile or yieldable solid (polymer). The housing contains an ejection groove or ejection ports (Fig. 1). If the piston is impacted, such as in a collision, the other end of the piston forces the ductile or yieldable solid through the ejection groove or ports, thereby absorbing much of the crash energy. The specific application for this technology investigation was an SEM shock track for the mounting of seats in rail passenger cars. In the event of, for example, a head-end or rear-end collision, the SEM shock track mounting would provide controlled acceleration and deceleration of the seat assembly. Although rail passengers do not wear seat restraints, the controlled acceleration-deceleration would provide some protection to passengers thrown into the back of the seat in the event of a head-end collision. In the event of a rear-end collision, the shock track would absorb much of the energy forcing the seats to the rear. The shock track would also reduce the likelihood of the breakaway of seat assemblies. Tasks included the identification of relevant railcar seat crashworthiness specifications (FRA, APTA, overseas), the design of the SEM crash energy absorption system for the seats and for an impact barrier, fabrication of an impact test Bogie vehicle equipped with railcar passenger seats and an instrumented test dummy, and a series of crash tests. These SEM energy absorbers were incorporated into the floor and wall attachments of passenger seats mounted on a Bogie crash test vehicle (Fig. 4). The rear seat of the two-seat test vehicle contained three test dummies, one of which was instrumented to record the dummy's secondary impact loads with the forward seat when the test vehicle impacted a barrier. Comparison of impact data (e.g., head impact and femur load values), with and without the SEM shocks revealed no significant differences in injury levels. The SEM shocks used in both the seat attachments and the impact barrier performed in accordance with the design specifications. Thus, the lack of reductions in injury levels was not due to any failure of the SEM shocks. It was due to several other factors, including the relatively high velocity differential between the seat and test dummies at impact; and the relatively high seat mass that needed to be accelerated by the colliding test dummies (both of these factors contributed to the high initial spike loads). But the primary reason there was little variance in the load performance between the SEM-modified and stock seats was due to the seat structures, which were designed to yield under the impact loading as defined in the current passenger seat specifications. So the seats underwent some level of yielding even with SEM shock mods. If a stiffer test seat model had been employed in this study (HSR-45), there likely would have been more discernable injury load improvements with the SEM shock absorbers.

KEY WORDS: High-Speed Rail; Crashworthiness; Crash energy absorption; Railcar passenger seats; Solid Ejection Material.

TABLE OF CONTENTS:	<u>PAGE</u>
Acknowledgments	2
Abstract and Keywords	3
Executive Summary	5
Background and Objectives	6
Idea Product	7
Concept and Innovation	7
Investigation	8
Review of Rail Passenger Seat Specs	9
Review of Rail Passenger Seat Studies	11
Review of Aircraft Passenger Seat Specs	13
Design and Fabrication of Bogie Crash Test Vehicle	13
Design, Fabrication and Static Testing of SEM Impact Barrier	14
Stress Modeling of Test Hardware	19
Design, Fabrication and Static Testing of SEM Seat Shocks	19
Test Results from Seat Impact Tests Conducted at TTI	21
Test Summary:	24
Conclusions:	33
Plans for Implementation:	33
References:	34
Glossary	35

EXECUTIVE SUMMARY:

This project investigated a new type of crash energy absorption method for railcar passenger seats. The goal is to reduce the severity of casualties to passengers involved in passenger train accidents. This new energy absorption method employs the SEM (Solid Ejection Material) shock technology. This technology is similar in concept to hydraulic shock absorbers, except that instead of a relatively low viscosity fluid being forced through a calibrated orifice, a very high viscosity semi-solid plastic or rubber material (e.g., polymer) is forced through a slot or orifice similar to squeezing toothpaste from a tube (See Figure 5). Forcing this material through a slot or orifice consumes substantial amounts of crash energy. The purpose of this project was to incorporate these SEM energy absorbers into the wall, floor and seat attachments of railcar passenger seats. In the event a passenger is thrown forward in a train accident and impacts the seat ahead, for example, the SEM devices would be designed to absorb some of the impact loads and thereby reduce the impact loads on the passenger. The amount of loading absorbed can be controlled by varying the dimensions of the SEM device (e.g., slot dimensions and piston diameter) and by varying the hardness (durometer) of the Solid Ejection Material. Prior to this research, SEM technology had only been tested in large-scale crash absorption applications (e.g. low-speed bumper shocks on full-sized pickup trucks and high-speed highway impact barriers).

These SEM energy absorbers were incorporated into the floor and wall attachments of passenger seats mounted on a Bogie crash test vehicle (Figure 8). The rear seat of the two-seat test vehicle contained three test dummies, one of which was instrumented to record the dummy's secondary impact loads with the forward seat when the test vehicle impacted an impact barrier. This impact barrier also used SEM shocks to provide the controlled deceleration of the crash test vehicle in accordance with the seat test specifications. Comparison of impact data (e.g., head impact and femur load values), with and without the SEM shocks revealed no significant differences in injury levels. Thus, the use of SEM technology for this specific application did not achieve the desired results. However, the SEM shocks used in both the seat attachments and the impact barrier performed in accordance with the design specifications. Accordingly, other applications of this technology are now being considered.

Based on review and analysis of the test data, there may be a simple explanation for the lack of an improvement in the personal injury numbers. There is a good analogy of two potential crash load environments that are experienced in current automobile designs; one being a seatbelt and the other being an airbag. A person has very little travel before contacting the seatbelt, so the load density can be high (e.g. high loads on a small area of belt). This is due to the person being caught early in his or her travel, so there's not a significant velocity difference between the person's body and the seatbelt. This results in a lower initial load spike and a more constant overall g-loading to the belt and person throughout the crash event. Belted occupants are essentially another part of the seat structure, so they will experience the same crash loads as the seat, which would be 8-g's max if the specified triangular crash pulse used in these tests is experienced. In such a crash load environment with belted passengers, there would probably be little need for shock modified seats since such systems would only reduce the relatively low 8-g spike load. This HSR-45 study involved the "typical" railcar crash environment, where the railcar passengers are not belted to the seat. This resulted in a completely different load history being delivered to those unbelted passengers. Such unbelted load environments deliver much higher spike load decelerations to the passengers' bodies.

Compare this now to an unbelted occupant. If a car is involved in a moderate- to-severe collision and the occupant is not belted in, then the "hard-constraint" from a seatbelt needs to be altered to a "soft-catch" environment (low loading over a large area) that is currently supplied by an airbag. Such systems help to reduce the initial load spike values. So instead of having a small, yet high load area, like a seatbelt or an SEM seat shock; a large and soft load area is needed to catch that unbelted passenger. A soft-catch surface is needed since the change in velocity between the person and the seatback has increased from essentially zero, in the hard-constraint seatbelt model, to 15 mph or 17 mph, in the unbelted rail passenger model. So the reason the SEM seat shocks didn't provide a marked improvement in head and femur load values was essentially due to the initial impact environment (e.g. dummy's first contact with the seatback in the first 5 – 7 milliseconds) remaining about the same in seat tests with and without SEM shocks. The reason the test dummy experienced about the same initial contact loads was due to the relatively high inertia or mass of the seat (approx. 140 lbs.). Thus the dummy's initial contact with the fiberglass seatback was close to being unaltered between a stock and shock modified seat. To reduce the head-impact loads, the fiberglass seatback itself would need to be more like an airbag, i.e., it needs to be soft and/or giving enough to reduce those initial load spikes. By making a softer surface the initial load spikes would be reduced, but it should be noted that while the majority of the peak head impacts measured by the instrumented dummies occurred in the initial load spike, some peak impacts occurred after the initial load spike (Figs. 21.5 & 21.7; note the seat broke free in Fig. 21.3 so it's not considered). Therefore these remaining loads, after the initial

load spikes, could be controlled by the yielding of the seat structures and/or displacement of the SEM seat shocks, thereby possibly reducing the later g-load history and kicking the peak impacts back to the region of the initial load spike. Thus, a notable improvement in the seat's head and femur load performances could be obtained if some type of soft padding or improved fiberglass seatback (in terms of its yielding) especially near the top of the seat back, could be added to the seat design. Such a seat back change could maintain the seat's current steel framework, while probably not requiring an SEM seat shock.

Of course concluding that there is no need for SEM seat shocks that would help "catch" unbelted passengers assumes that there is no advantage in having a seat with a more rigid steel framework (the service life for such seats may be improved), while substituting SEM shocks for the yielding performance of the existing steel frame design. Lastly, this does not remove the possible need for SEM seat shocks for other applications. For instance, vertical load seat shocks for emergency helicopter landings or for the mitigation of mine blast loads that military vehicle seats can be exposed to are both analogous to the seatbelt application, in that they are also a hard-constraint model. The passengers remain seated with their thighs and posteriors in contact with the horizontal seat pad throughout the vertical shock load event, so there is never any free flight travel to necessitate a shock system with soft-catch characteristics. These events can be categorized as falling into a hard-constraint, yet controlled displacement model, which is a perfect match for SEM seat shocks capable of mitigating the severe g-loading from such crash and blast events.

The investigative approach for this project included a review of existing railcar passenger seat specs, both domestic and foreign; passenger seat test methods and test results; the design, fabrication and static testing of the SEM seat shocks and the supporting test hardware (e.g. test vehicle and impact barrier). A series of crash tests were then conducted. The initial series revealed the need to redesign both SEM seat shock types, i.e., wall and floor models. The initial seat shocks were designed to displace under a greater and more sustained shock load than the loads experience in the initial test series. The design of these initial seat shocks was based on crash test results using older seat designs some of which (6) did not meet the newer APTA SS-C&S-016-99 seat spec (2). In the more aggressive, full-scale railcar crash test (1) the M-Style seats did fail, but the impact speed was 35 mph vs. the spec 21.9 mph; so at the time of this HSR-45 test effort it was assumed that the M-Style seats didn't meet the seat spec. It was later learned that additional sled testing was conducted on the M-Style seat, using the spec 8-g x 250 ms load conditions (14), and all of the human injury limits for the three 50th percentile male test dummies were within spec limits. The seats used in this project, however, were known to conform to these new specs. As a result, the newer seat structures did all of the yielding and energy absorption, so the SEM seat shocks experienced very little displacement due to their higher restraint load performance.

The SEM shocks were redesigned based on the results of the initial test series. Another series of crash tests were run using the redesigned SEM shocks. The redesigned SEM seat shocks performed as planned. There were substantial displacements in both the wall and floor shock models, i.e., the solid ejection material was extruded through the ejection groove. Analysis of the dummy head accelerometer and femur load cell data, however, provided no indication that the redesigned SEM shock made any major contribution to the reduction of the head and femur load values of the instrumented test dummies.

BACKGROUND AND OBJECTIVES:

The major goal of this study was to see if a new type of crash shock technology, Solid Ejection Material (SEM) crash shock technology, could be incorporated in railcar seat designs to reduce the impact injuries experienced by unbelted rail passengers during railcar derailments or collisions.

Prior to this study, no testing had been performed on smaller impact load applications of this SEM technology, such as passenger seat shocks. There had been several large impact tests using large drop weights and full sized vehicles, but even the smallest loads experienced in the past SEM shock tests were five times greater than the load projections for the highest seat shock loading. These previous tests included drop tests using impact weights of 500 lbs dropped from 30 feet. The drop weight obtained speeds of 30 mph. Several high-speed vehicle impact tests were conducted, including an SEM shock system mounted on the front of a ¾-ton pickup truck that struck a barrier at speeds ranging from 3.5 to 7.5 mph. Also, a 1700 lb crash test vehicle impacted a barrier equipped with SEM shocks at speeds up to 62 mph.

Based on the Principal Investigator's knowledge of the SEM technology, there did not appear to be a problem in downsizing SEM shock load performance to where restraint loads of 1,000 lbs_F to 2,000 lbs_F could be delivered. Based on the results of the previous proof testing on SEM technology and its potential for other applications, the High-Speed Rail IDEA Program determined the potential worth of studying and testing railcar passenger seats that had been modified with the SEM shock technology.

IDEA PRODUCT:

The potential product resulting from this study would be a passenger seat SEM shock system that would provide a lower passenger crash load environment during a collision or derailment event. Many of the older seat models had very stiff and non-yielding seat structures that were not very “crash friendly”. This means the passengers’ bodies would absorb much of the Kinetic Energy if these seats remained attached and the seat structures experienced very little buckling or yielding. Also, some older seats have poor attachment methods, thereby allowing the free flight of the passengers into other, possibly more damaging, non-yielding structures (e.g. walls, poles). SEM seat shocks could potentially solve the breakaway problem and reduce those spike loads and thereby take on a greater percentage of the energy dissipation.

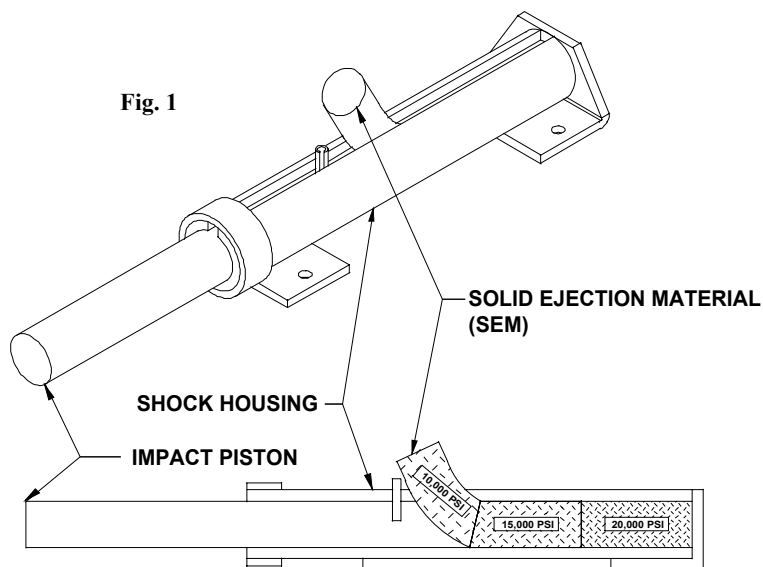
Some of the newer seat models that already meet the APTA (American Public Transportation Association) seat specification [APTA SS-C&S-016-99 (2)] through the yielding and crushing of their current seat structures may not need SEM seat shock mods. This was clarified after the review of the test data, where there was very little reduction in the peak injury levels. Although, while there was not a great improvement in the overall crash load performance of a production model seat that meets the APTA spec, this does not eliminate the option of substituting SEM shocks for some of the buckling and yielding structures in the current seat design. For example, could there be any improvement in the overall service life of the seat if the current lightweight frame structures were replaced with more substantial structures and SEM shocks were substituted for the current yielding and buckling structures?

While there is a potential need for SEM shocks in a non-yielding seat design, there is probably more of a need for a soft padded seat backing to reduce the initial contact loads of the passenger’s head, knees and chest. This does not mean that there are not other SEM seat shock applications that would prove to be a clearer safety improvement. If a vehicle occupant remains seated and there is no “free-flight” involved, such as in vertical crash or blast load events, then there is still a need to reduce the overall pulse loading, from the high initial load spikes of 20-g’s to 30-g’s, or more, down to more survivable levels of 7-g’s to 10-g’s. Such performance levels have already been tested and proven in a SEM drop test effort, where an initial load spike was reduced from its 45-g peak, down to more manageable levels of 17-g’s to 9.3-g’s.

Two systems were actually tested in this study, i.e., the SEM seat shocks *and* the SEM impact barrier that was used to deliver the deceleration pulse to the Bogie test vehicle as specified in the APTA spec. Both shock systems functioned very closely to their desired design performance. In fact, the impact barrier’s spec 8-g by 250 millisecond triangular crash pulse versus the actual crash pulse was very close to the spec overlay (see figs. 10.1 to 10.9). Such performance tailoring in the few hundred lbs_F for the seat shocks and up to 35,000 lbs_F for the impact barrier helped prove the appreciable performance range of the SEM shock technology and could perhaps open the doors to more substantial rail impact load applications (e.g., railcar couplers and draft gears, collapsible railcar structural components).

CONCEPT AND INNOVATION:

The SEM (Solid Ejection Material) shock technology basically employs the same high pressures that are present in the injection molding process of plastic and elastomer (e.g. polymer) parts. Such polymer flow pressures can range from 2,500 psi up to 35,000 psi, depending on the injection material type, material temperatures, flow passage area and lengths (e.g. cross sectional area of flow tube) and the complexity of the injection molding die’s geometry. The typical SEM shock consists of a simple piston assembly, a plastic or elastomer flow medium of different properties (e.g. stiffness or durometers, fiber inclusion, etc.) and a shock housing with perforations (e.g. staggered hole patterns) and/or a continuous slot or ejection groove (Fig. 1). Because of the unique type of flow medium employed, solid polymers, there are no fluids or gases to leak. Therefore, no fluid seals are required for SEM shocks. Even though these solid flow mediums have some level of fluid properties when exposed to extreme pressure loads; these solid or “semi-fluid” mediums are still so viscous they have difficulty passing through tight openings or passages (such as around a loose fitting piston). So tight tolerance controls which are required for pneumatic and hydraulic shocks to assure no leakage, are not needed. Loose tolerance controls help to reduce the overall fabrication costs, since there are fewer part rejections and a broader range of machine tool types that can produce these loose-tolerance parts. Another advantage to the technology is the simplicity of the primary manufacturing methods. Most of the parts are simple roll-formed or extruded parts, with little if any final prep work other than the cutting of some parts to length and some limited welding. Again, this keeps the



overall manufacturing costs low. Lastly, the SEM technology possesses the option of extreme pressure operation, unlike the limits for most hydraulic shocks. The top pressure extremes for most production model hydraulic shocks top out at 10,000 psi, whereas SEM shocks can hit pressures of 35,000 psi or more. So if a large impact application required a 5.0" ID SEM shock operating at 35,000 psi, for a total restraint load performance of 687,223 lbs_f, then a comparable hydraulic shock would need to have a 9.35" ID, or nearly double the dimensions and probably more than three times the weight and probably many times the costs.

Another unique SEM feature that is not even an option with hydraulic and pneumatic shocks is the "side-access" feature, to the SEM piston assembly. The side-access feature is an option of the SEM shock housings with the continuous ejection groove (Fig. 1). Essentially there is now the option of designing structures that attach to the piston through the ejection groove, which results in lighter-weight structures and essentially unlimited travel lengths in some applications. All of the SEM shock systems in this study, the impact barrier and both seat shock models, used the side-access feature. To help clarify some of the advantages of this feature, the standard hydraulic shock is over double its available travel length when it is fully extended. So if 12.0" of piston travel is needed, then the overall extended shock length would be slightly over 24.0" (e.g. structures such as seal end caps and piston end attachment structures will all add to that 24.0" length). As a comparison, the SEM shock housings used in the impact barrier were 78.0" long. Of that 78.0" length, the impact piston assembly length took up 7.0" and the two end piston assemblies each removed an additional 2.0" of space. But even with these incursions the SEM impact barrier housings still had 67.0" of available travel. So instead of needing a 67.0" long piston to get that 67.0" of travel, only 11.0" of piston structures were needed to obtain those 67.0" of travel. Note: that 67.0 inches could have been 67.0 feet if needed and this particular barrier design still would have only required 11.0" for the piston structures. This same feature allowed for several improvements to the seat shock models, such as very high moment loading (torque) since there are no long cantilever beam structures (e.g. standard pistons) which are present in conventional shock designs. Also, the SEM seat shocks had dual travel pistons to take on both forward and aft impact loading, this would have been a difficult feature to replicate using conventional shock designs; and again, the compressed shock length for the available travel (e.g. Shock Length Extended to Available Travel ratio = L_E/A_T) will always be greater than 2 for standard, unarticulated, shocks (e.g. $24.0"/12.0" = 2.0$ for the above standard shock example with a 12.0" piston); whereas SEM shocks that employ the side-access feature will always be less than 2.0 and with larger systems will start approaching 1.0 (e.g. SEM impact barrier used in this study; $L_E/A_T = 78.0"/67.0" = 1.16$). Essentially what this starts to approach, as the overall SEM shock length increases, is the elimination of the piston structure and its weight *and* its cost.

One last characteristic of the SEM technology that should be touched on, which is critical to crash safety systems, is system reliability. This is another area where SEM shocks score high. The reason for this is due to the SEM shock's very low part count, which typically only has 3 parts, whereas the typical hydraulic shock may have 20 parts. So to do a rough reliability estimate (e.g. of course in the real world part reliabilities vary between part types) assume each part has 99% reliability (e.g. 1 part fails out of 100); then an SEM shock assembly with 3 part would have a 97.03% system reliability (e.g. 0.99^3); whereas the standard shock, with its 20 parts, would have a 81.79% system reliability (e.g. 0.99^{20}). Of course the number of parts has a play in system reliability but so do the type and complexity of the parts themselves. Because of the basic function of SEM parts there really are very few possible failure modes; the ejection material properties may be altered due to a passenger compartment fire (e.g. the material maybe be softened); or there could be a problem with QA, Quality Assurance, at the point of manufacture, such as incorrect ejection ports sizing or the wrong durometer material is installed; but all of these possible failure modes are very rare and very controllable. Compare this now to a conventional seat's, standard steel framework, which is designed to yield under severe loading. After a few years of heavy operations the seat frames could fail at lower crash loads due to fatigue cracks. These fatigue cracks would be due to the lighter-weight construction of the seat's steel frame, to assure the framework will yield under crash loading. So it may be better to build a heavier, less yielding seat frame with some form of shock mod, to avoid fatigue failures. Also, if pneumatic or hydraulic shock systems are employed then the overall system reliability, over many years of operations, could be quite low. Some of this is due to the larger part count (giving that rough 81.79% value) but primarily, those low reliability numbers will be due to fluid leakage, where a conventional shock will be inoperable if enough fluid is lost. Of course very reliable conventional shocks can be produced, since the typical suspension shock for a car can last for years, but all of the reliability improvements (e.g. tighter tolerances, etc.) add to the manufacturing costs.

As a side note, the SEM technology was tested before the initiation of this (HSR-45) study. Two high-load drop test efforts and two full-scale vehicle impact tests had been completed before HSR-45 began. A 2001 SAE report (13) has complete test data regarding the SEM shock performance in these earlier test efforts.

INVESTIGATION:

The basic investigative approach included the design, fabrication and testing of a prototype system. After initial completion of these tasks, the test data revealed the need to redesign and then retest the SEM shock system. As with most study plans, there were changes in the plan of attack as the study evolved. For instance, the initial test plan involved the use of railroad tracks and rail-type vehicles for the crash test platform, but because of the size and resulting costs of full-sized railcars and locomotives, this option would exceed the project budget. As a result, this plan evolved into the use of a smaller Bogie test vehicle equipped with highway tires. Other changes also evolved throughout the test effort such as the impact velocity of the crash test platform (Bogie vehicle). Some earlier tests used impact velocities of some 30 mph, whereas the requirements in the APTA seat spec resulted in impact velocities of 21.9 mph (Note: 23.5 mph was the velocity used to allow for the additional impact sled mass). Even though the current spec required a less aggressive impact pulse, it was the current industry standard that new seat manufactures had to adhere to, so the lower impact velocity was employed in all tests.

The following is an overview of the HSR-45 Study Tasks.

Stage 1

- Review any existing modeling, analysis, and crash test data for passenger seats.
- Collect and analyze any international spec and/or test data for HSR seating.
- Analyze specs and performance data for seating systems outside of rail applications (aircraft, military systems) that are designed for impact or shock loading.
- Obtain current railcar passenger seat designs and FRA, APTA and other spec requirements for seats.
- Convene a Panel with expertise in the crashworthiness analysis of rail passenger equipment, and/or the crash testing of such rail equipment or similar transportation hardware, to provide technical support and guidance regarding commercial applications.

Stage 2

- Design SEM shock track and piston assembly to interface with existing train seating.
- Design Bogie vehicle for test seat mounting.
- Design SEM impact barrier to deliver spec deceleration pulse.
- Stress model all SEM components and supporting test hardware.
- Computer model potential test performance of prototype systems (was not doable with available resources).
- Conduct static load tests on SEM seat shock designs and modify as needed.
- Develop test plan.
- Stage 3 tasks undertaken in Stage 2 - Bogie vehicle completed, steel SEM impact barrier components completed, SEM seat shocks completed.

Stage 3

- Fabricate SEM test components, much of which was completed in Stage 2.
- Conduct static tests on impact barrier before Texas Transportation Institute (TTI) test effort.
- Run full scale Bogie-barrier-seat impact tests at TTI's test facilities.
- Analyze test data.
- Based on the need for additional testing, due to the unforeseen seat shock performance, a continuation of the HSR-45 study was approved to redesign and retest the seat shocks.

Stage 4

- Redesign seat shocks to deliver lower restraint load performance.
- Fabricate and static test new seat shocks and revise as needed.
- Determine if any modifications are needed in current impact barrier performance.
- Setup test plan for the next TTI test.

Stage 5

- Conduct Bogie impact tests at TTI using the modified seat shocks.
- Analyze test data.
- Prepare final report.

Discussion of these tasks will be presented in sequence, when appropriate. Some of these tasks overlap between stages and the test data also overlaps between the two TTI/SEM test efforts. Some discussions are, therefore, grouped rather than presented in stage sequence. For instance, the design and actual fabrication of a particular piece of test hardware will be grouped even though those actions were taken in separate stages (Stage 2 and 3). All of the test data from the Nov. 2004 test effort (Stage 3) will be grouped and discussed in parallel with all of the test data from the Nov. 2005 test effort (Stage 5). This should reduce the fragmentation of the discussion and keep the redundancy to a minimum.

Review of Rail Passenger Seat Specs:

Most of the research into past passenger seat tests was found through internet searches and recommendations from the Panel members who had been involved in past crash test studies. Generally, the majority of the available data was from U.S. agencies and test labs such as FRA, DOT, FAA, U.S. Army, and Volpe. Some of the reports involved aircraft-type seating but the main focus was to locate test data and seat specs related to railcar type seating. The goal of this research was to quantify the impact speeds, railcar deceleration history and the allowable injury levels for passengers, so that these parameters could be duplicated in the full-scale HSR-45 crash test effort.

To provide a useful gauge on the potential injury levels that a train passenger might experience during a collision, the following table (3) from the American Association for Automotive Medicine (Pike 1990) gives a good overview.

TABLE 1 AIS CODE, HIC, AND CHEST DECELERATION

AIS Code	HIC _{36ms} (11)	Head Injury	Chest Deceleration	Chest Injury
1	135-519	Headache or dizziness	17-37 G's	Single rib fracture
2	520-899	Unconscious less than 1 hour; linear fracture	38-54 G's	2 to 3 rib fractures; sternum fracture
3	900-1254	Unconscious 1 to 6 hours; depressed fracture	55-68 G's	4 or more rib fractures; 2 to 3 rib fractures with hemothorax or pneumo-thorax
4	1255-1574	Unconscious 6 to 24 hours; open fracture	69-79 G's	greater than 4 rib fractures with hemothorax or pneumo- thorax; flail chest
5	1575-1859	Unconscious more than 24 hours; large hematoma	80-90 G's	Aorta laceration (partial transection)
6	>1860	Non-survivable	>90 G's	Non-survivable

Depending on the AIS (Abbreviated Injury Scale) Code and the corresponding HIC (Head Injury Criteria-defined later) and chest deceleration values, one can see the level of injuries that a passenger may experience. Of course these injury levels depend on the seat separation, the energy absorption performance of the forward seat and the type of energy absorption performance (e.g. soft-catch). A railcar seat spec was found, APTA SS-C&S-016-99 (2), which will be discussed in more detail. These APTA requirements actually fell into the AIS code category with a value of 3. It can be seen that even if an AIS value of 3 can be achieved, there will still be some fairly serious injuries sustained by the passengers (e.g. unconscious 1-6 hours, rib fractures, etc.). This data shows the need to improve a railcar seat's crash energy performance beyond the current seat spec requirements, if possible. As an aside, there are revised and newer versions of the APTA SS-C&S-016-99 spec but to the Principal Investigator's knowledge there have been no changes to the spec requirements for a 50% male; those values being, HIC_{36ms} = 1000, chest deceleration 60g over 3 ms, Axial Femur load 2,250 lbs. The APTA spec addresses both the injury levels sustained by passengers and also seat structural requirements to increase the likelihood that seats remain attached during a severe passenger train crash event. The spec requires that the seats must stay attached while experiencing an 8-g max by 250 ms duration triangular crash pulse.

As to international specs for railcar passenger seats, little was found in multiple searches of Japanese rail websites. It was assumed that the absence of Japanese websites related to the rail industry was probably due to a lack of English translations of the pertinent web pages. Although, after a review of European and Canadian websites and communication with certain individuals, a likely explanation is that the United States may have the most aggressive safety specs for railcar passenger seats. The less aggressive seat specs for the European market was unexpected, especially considering that some euro trains are moving at 300 Km/hr (186 mph) and some maglev trains have top speeds of 300 mph!

The Canadian spec (4) requires a securement of fixed passenger seating designed to withstand a 5-g longitudinal, 3-g lateral and vertical forces, with one 185 pounds (83.9 kg) passenger in each seat, without failure of seat attachments. No European railcar seat requirements were located but the Technical Director at the Cranfield Impact Centre in Bedford England recalled that in the "Safetrain" project there was a quasi-static test requirement equivalent to a 5g load and he noted that this spec was "clearly inadequate for real-world conditions" in terms of the relatively low breakaway accelerations for British railcar seating.

Domestic Rail Passenger Seat Spec (APTA SS-C&S-016-99):

The domestic railcar passenger seat spec, APTA SS-C&S-016-99 has already been touch upon but a more detailed breakdown is needed to convey the test parameters and performance goals that were employed in the HSR-45 study.

Impact Barrier Performance – The APTA spec had a number of seat component tests that the seat manufactures have to adhere to, such as backrest static load tests and armrest strength tests, to name a few. It was known that the stock passenger seats would meet all of the component part requirements and that the only area where the SEM technology could possibly improve the current seat structures would be in the addition of floor and wall mounted SEM seat shocks, to share some of the seat's current bending and yielding loads. Therefore the only pertinent spec requirements for the HSR-45 study would be the crash pulse delivered to the test seats and unbelted test dummies, and the resultant load environment of the test dummies' body parts (e.g. Human Injury Levels). The APTA

spec did have a crash load environment defined, which would simulate the deceleration environment of an aggressive train crash or derailment, that being a triangular crash pulse with an 8-g max deceleration and a 250 ms duration (Fig. 2). To achieve that deceleration pulse the Bogie test vehicle would need to have an initial impact velocity of 21.9 mph and the SEM impact barrier would need to be tailored to supply an ever increasing restraint load, up to 125 milliseconds (ms) and then drop off for the remaining 125 milliseconds travel time.

If the correct triangular crash pulse could be delivered to the Bogie assembly, then the next task and of course the primary goal of the HSR-45 study, would be the measurement of the Human Injury Levels experienced by an unbelted passenger in a railcar crash event. As a side note, it was known that an “ideal” triangular crash pulse was difficult to achieve even with past test platforms (ref 7 - plot on pg 21) which were more controllable, although it was also known from past SEM drop tests that the SEM technology was controllable enough to achieve a reasonable deceleration pulse, so that comparative seat performance data between each seat test could be achieved. Since the railcar passenger seats already met the current APTA seat spec, it was thought that the SEM shock mods would further reduce these loads, thereby improving their current crash performance. The following table summarizes the maximum crash load values for the head, chest and legs for a “typical” 50th percentile male weighing 168 lbs.

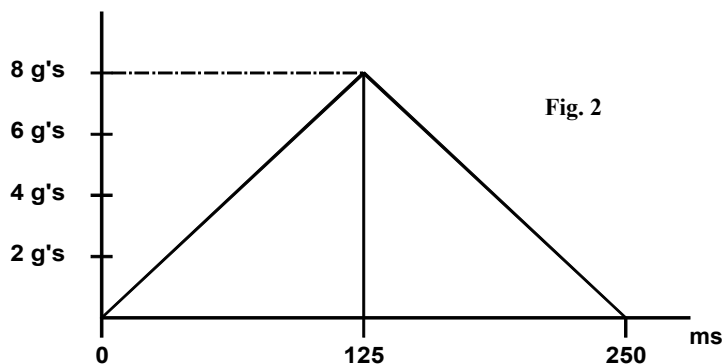


Table 2 - Human Injury Limits for 50% Male (APTA)

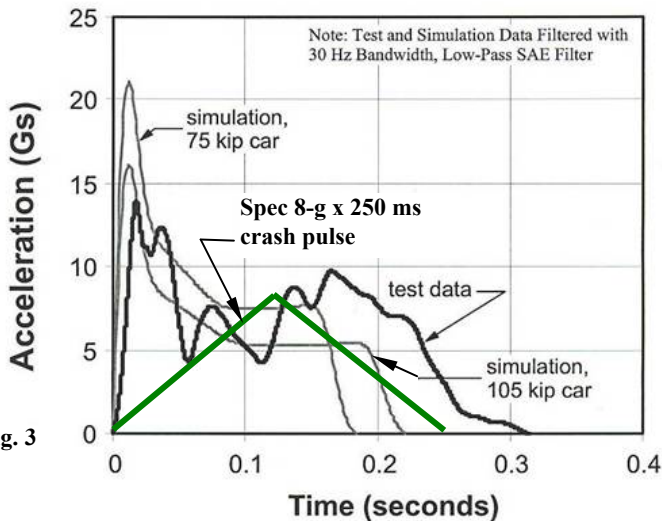
Criterion	Maximum Value
HIC _{36ms}	1000
Chest acceleration	60g over 3ms
Axial Femur load	2250 lbs. (10,000 N)

The HIC (Head Injury Criteria) value takes into account the deceleration and duration delivered to a passenger’s head upon contact with the forward seatback.

Review of Rail Passenger Seat Studies:

The primary report data that was used in the design of the SEM seat shocks was taken from three DOT/FRA reports (2, 6, 7, note 2 and 6 covered the same test effort). Both of these railcar seat crash tests [Single Passenger Rail Car Impact Test Volume II: Summary of Occupant Protection Program (1); Single Passenger Rail Car Impact Test Volume I: Overview and Selected Results (5); Crashworthiness Testing of Amtrak’s Traditional Coach Seat (6)] experienced some seat detachment of some of the test seats. While neither test effort was an exact match with the HSR-45 study, there was some very useful data obtained from all three test reports, which helped in the design of the SEM shock systems (both impact barrier and seat shocks). While at the time of each TTI/SEM crash tests, the above test reports were used for seat shock sizing and general test planning. While not an exact match, some of the test data did assist in the general design. There was another series of tests (14) which was learned about at a later date, and the data from this more recent test effort was a better match to this HSR-45 study effort.

Comparing the HSR-45 study and the 1999 DOT/FRA full scale railcar crash test (5); the 1999 study used a much higher impact speed (e.g. 35 mph versus a 21.9 mph impact velocity, the latter of which is needed to deliver a spec 8-g by 250 ms triangular crash pulse). Therefore, a more aggressive impact pulse was experienced (Fig. 3) by all three seat configurations in the 1999 DOT/FRA study. Note: The plot shown in Fig. 3 was taken from the 1999 DOT/FRA study but it



was modified through the addition of a spec triangular crash pulse, for comparison purposes. Of course this test used a single railcar and a higher impact speed than the velocity used in the HSR-45 study, but it should be noted that there are some test cases where the crash load environments were more aggressive than the current spec requirements.

In the 1999 DOT/FRA study there were two total structural failures of the seat assemblies, both of which were the three passenger model seats (1). One seat detachment occurred in the No. 1 seat setup, which used two M-Style commuter seats; the back one seated 3 unbelted 50th percentile male Anthropomorphic Test Dummies (ATDs) and the forward seat was used to impede the forward travel of the 3 test dummies at railcar impact. This seat configuration was the closest match to the test seat setup employed in the HSR-45 study (3 unbelted passengers, hitting a forward seat). The second failure occurred in the No. 3 seat set up, which used one rear facing M-Style commuter seat with three 95th percentile male ATDs placed in it. While this seat had the lowest impact pulse loading, due to the lack of free travel or free flight of the test dummies, since it was rear facing, the loading was still great enough to fail the floor attachments. The No. 2 seat was the only seat that didn't breakaway but it essentially dealt with 4 test dummies (3 of which were 95th percentile male ATDs), since it had two unbelted dummies in the rear seat and two belted passengers in the front seat. Also, this test seat had a modified seat back and attachments to handle the higher test loading, plus the two seats had a greater seat pitch (separation) of 41.0" versus the 33" used in the HSR-45 study. Although these test parameters were not an exact match of the test parameters employed in the HSR-45 study; at the time of the preliminary research study this was the only test data that was recovered. Plus, since this seat didn't breakaway it was thought to be the closest representation of the loading that would be experienced in the HSR-45 study. The following table gives the Human Injury Levels experienced by the test dummies in each seat configuration and that max x-loading along the longitudinal axis delivered to the floor attachments of all three seat configurations.

Table 3
Select Data from DOT/FRA *Single Passenger Rail Car Impact Test Volume II* (Reference 2)

Seat Test #	HIC _{36ms}	Chest (g's)	Left Femur (lbs)	Right Femur (lbs)	x-load max (lbs)	x-load max (lbs)
No. 1 (Failed)	202	14-g's	670	806	981 wall	2,239 floor
No. 2	854	27-g's	1,959	3,116	8,703 floor-1	8,588 floor-2
No. 3 (Failed)	N/A	N/A	N/A	N/A	1,556 wall	1,674 floor

Similar results in terms of seat breakaway occurred in a 1996 DOT/FRA railcar seat test (6), where 7 dynamic tests were run. The first seat test used a 5-g peak load; the second test seat underwent a peak loading of 10-g's and the remaining test seats employed the spec 8-g loading. At the time of these tests the seat was known as "Amtrak's traditional seat pair". These seats were capable of carrying 2 passengers. A brief quote from this report gives a good summary of the test results.

"The most critical failure observed was at the wall mount where the side bracket fastens the seat frame to the wall track. In every test, except 1 and 3, the side bracket failed to remain fixed in the wall track, allowing the seat to pivot about the floor pedestal. In two tests, the pivoting of the seat caused enough deformation of the floor track, breaking the track in one case, to allow the floor pedestal to separate from the track. In those tests, the seat was entirely detached from the test sled. In a collision, a loose seat, weighing over 200 pounds, could be a serious hazard to passengers." (6).

Note: The reason the 1st and 3rd seats probably did not fail was due to the lower deceleration loading in the 1st test and the fact that only one test dummy was used in the 3rd test. Table 4 gives a similar test data summary as Table 3, but the data used was from the 1996 DOT/FRA test effort (6).

Table 4
Select Data from DOT/FRA *Crashworthiness Testing of Amtrak's Traditional Coach Seat*

Seat Test #	Peak Sled g's	HIC _{36ms}	Chest (g's)	Max Femur Load (lbs)	x-load inboard max (lbs)	x-load outboard max (lbs)
#1	5-g's	181.8	10.8	1035	1220.0	1450.7
#2 (Failed)	10-g's	133.1	18.0	1616	3537.1	1916.7
#3	8-g's	112.4	19.2	2202	2470.1	1646.1
#4 (Failed)	8-g's	179.3	19.7	1639	3193.9	1815.0
#5 (Failed)	8-g's	193.5	11.6	1293	2171.9	2165.5
#6 (Failed)	8-g's	41.3	11.8	1579	3467.3	2318.9
#7 (Failed)	8-g's	810.5	7.8	822	2575.3	2650.0

While the 1996 DOT/FRA test effort did use the spec crash pulse that would be used in the HSR-45 study, the earlier study still employed an older 2-passenger seat in their tests. Also, like the 1999 DOT/FRA test effort the majority of the seat attachments failed, which means the peak seat loading (e.g. x-loading) and Human Injury Limits (e.g. HIC, Chest g's, Femur Loads) would have undoubtedly been greater if the seats had remained attached at the wall. While not ideal load data for the HSR-45 study the test data was still valuable in sizing the SEM seat shocks. Therefore the load data from the second test run in the 1999 DOT/FRA study, along with the data from the third test run in the 1996 DOT/FRA study was used in the initial SEM seat shock sizing.

Review of Aircraft Passenger Seat Specs:

The 25.562 FAA spec has many similarities to the U.S. railcar seat spec (APTA SS-C&S-016-99). The two specs use the same test dummy spec requirements, such as the same HIC and femur loads limits (7). Where the specs depart is in the max g-loading that the seats must survive (e.g. 8-g train seats, 16-g aircraft seats), plus the crash pulse is more defined in the railcar seat spec (e.g. 8-g by 250 ms triangular crash pulse). Also, the railcar seat spec limits the max chest acceleration to 60-g's over 3 ms, but this requirement is not in the aircraft seat spec, due to the passengers being belted in. Instead, a number of seat belt performance requirements replace the railcar chest acceleration spec.

To help convey the advantage of high failure load seating, a U.S. DOT/FAA report discussed a study that modeled the substitution of 16-g passenger seats, for the stock 9-g seats used in place in past crash events (8). Twenty five aircraft accidents, which happen between 1984 and 1998, were modeled with seat upgrades from the 9-g seats to 16-g seats. In those 25 flights there were 1,423 fatalities and 527 serious injuries, but from the computer model, if the 9-g seats were replaced with 16-g seats, then 68 people (high statistical estimate) would have been saved, and 79 other passengers (high statistical estimate) would have avoided serious injury.

From such reports it can be seen that some improvements in the passenger seat energy absorption performance should be beneficial to the improvement of passenger safety.

It should be noted that other more aggressive shock loading of passenger seats was also studied, such as mine-blast loading of military vehicle seats and helicopter seating experiencing emergency landing loads. While these applications are also viable applications for SEM shock mods, the general crash model did not match the railcar seat model. For instance, in a mine blast event the peak g-loading is shorter and much more severe (9) (e.g. 31.4 g's over 7.0 ms); plus the peak decelerations are in the vertical direction (y-axis) instead of the horizontal (x-axis) direction; and lastly there is no unbelted free flight travel of the passenger, instead the passengers experience the vertical pulse load while remaining in the seated position.

Design and Fabrication of Bogie Crash Test Vehicle:

Several crash test vehicles or Bogie vehicle designs were considered, such as rail sleds, etc., but a final test vehicle design was not locked in until the Texas Transportation Institute (TTI) at Texas A&M had agreed to be the test facility. TTI already had a Bogie test vehicle, which employed a small automobile frame, with added stiffening framework and mass loading to model a vehicle undergoing and/or delivering high crash loads. After reviewing the existing TTI Bogie design it was decided that it would be too difficult to modify its framework to provide a large enough platform to mount a dual passenger seat configuration. So it was determined that a substitute or newly-constructed test platform was needed.

The Principal Investigator had reviewed past IIHS (Insurance Institute for Highway Safety) reports and a potential test vehicle design that had been used by the IIHS in a number of its side impact tests was selected. This design appeared to be a good test platform for this TTI/SEM seat test effort. The IIHS test vehicle (10) had a large unobstructed top surface area, with enough area to easily receive the two SEM-modified test seats.

Although after contacting some IIHS personnel it was learned that the IIHS side impact vehicle was not a unique IIHS design, but was an NHTSA test vehicle design, which was called the Moving Deformable Barrier (MDB). The appropriate drawings for the MDB were purchased and modified to construct the TTI/SEM Bogie test vehicle.

The original MDB drawings came from the (CFR) 49, Part 587, Subpart B, specification. While the original design weighed in at 3,300 lbs, a good percentage of the weight came from the addition of numerous ballast plates. It was assumed that the MDB's removable ballast plates allowed for a change in vehicle mass to model a range of colliding vehicle types. Although for the HSR-45 study, a total vehicle weight of 4,000 lbs was projected as being

needed, and since TTI already had an existing lightweight Bogie vehicle, it was assumed that there was no need for removable ballast plates on the new Bogie to make it lighter. Therefore, it was thought to be prudent to make a more substantial and heavier vehicle frame (Fig. 4). This was done by replacing the 3.0" x 2.0" x 0.25" spec rectangular tubing, with its numerous ballast plates, with a heavier vehicle frame constructed from 4.0" x 4.0" x 0.25" square tubing, in addition to only *one* 0.75" ballast plate, which would then



Fig. 4

be welded to the top of the new Bogie's framework. Also, the original MDB design had no real-time steering (e.g. the front wheels had to be set by removing and resetting bolts) plus no braking action. These features were determined to be essential for the TTI/SEM Bogie, so the vehicle's two axles consist of a steerable mining vehicle front axle, with a steering gear box and accompanying steering mechanisms; and the rear axle was a trailer axle with an electric brake assembly. The rear axle's load capacity was rated at 3,500 lbs. Both axles had matching 5 x 4.5" bolt patterns so that they could receive the same 15" wheels. An electric brake switch was added near the side mounted steering wheel and TTI supplied a radio controlled switch to activate the brakes if, during a test run, emergency braking was required.

There were several structures that were added to the Bogie frame for the function of seat mounting and other component support/mounting (e.g. load cells) and these structures also provided the needed ballast to achieve the vehicle target weight of 4,000 lbs (minus 510 lbs for test dummies and approximately 280 lbs for seating). The 0.75" ballast plate was added to provide the needed weight addition of some 800 lbs but also to serve as the vehicle floor. The ballast plate was sized after quantifying the weight of the unchangeable vehicle structures (e.g. axles, wheels, steering box, etc.) and set test components (e.g. seats, dummies, load cells). The Bogie vehicle also had a wall structure framework constructed to simulate a railcar wall, thereby allowing the attachment and support of the seats' elevated wall mount side. Finally, a forward plate structure (plywood and rubber padding) was added on the Bogie vehicle's front impact frame. These structures helped to distribute the load and reduce the impact ringing or vibrations, which could interfere with the accelerometer readings. Lastly, the addition of a plywood floor spacer was also needed because of the increased seat height that was added by the SEM floor shock. This floor spacer was needed to assure the proper placement heights for the test dummies' feet.

Figure 5 shows the midsection of the ballasted Bogie, which was used in the first three crash tests to check the performance of the SEM impact barrier.

Since there were no test seats or test dummies installed in the first three impact tests, ballast plates were substituted to make up for the 700 lbs weight differential. While the photo does not show the detail of all of the parts, it does give a good view of the location of the various test parts and instruments. For instance, there were six, single-axis load cells installed in the Bogie framework, all of which were rated to accurately measure loads up to 10,000 lbs_f max. The four load cells in the back and front of the SEM seat shocks measured the vertical loading; and the remaining two load cells to the far right, in Fig. 5, measured the forward loading. The reason six single-axis load cells were employed instead of four, 3-axis load cells, was due to the considerable cost difference between the two load cell types. The single-axis models were still expensive, approximately \$700/unit but their cost was about 10% of the cost of the 3-axis models. By making this load-cell compromise, some of the load data was probably slightly skewed to higher load values. This was due to the slightly heavier channel steel mounting beams, to which the seat shocks and load cells were attached; in addition to some horizontal frictional losses between the vertical load cells bolts and the channel steel. It was projected that these load shifts should be well within 10% of the actual loads, which was well worth the cost difference for this stage of testing.

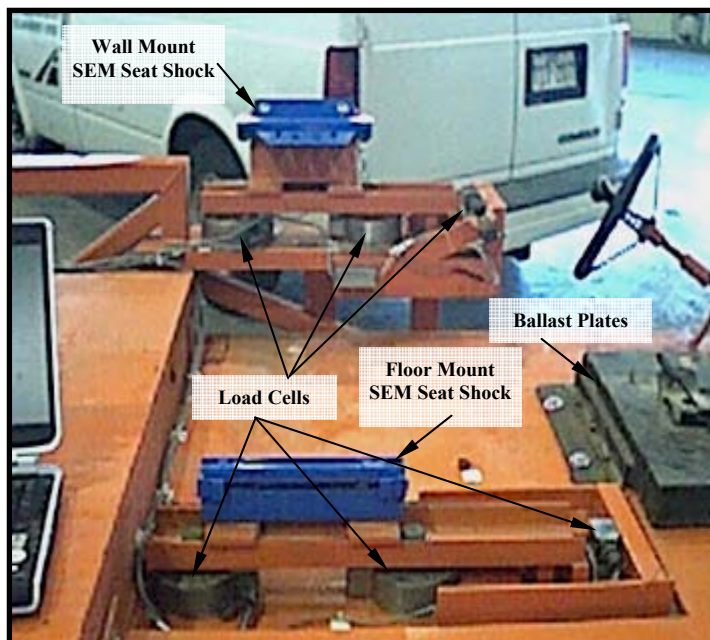


Fig. 5

Design, Fabrication and Static Testing of SEM Impact Barrier:

While the major focus of the HSR-45 study was the impact load testing of stock railcar passenger seats that had been modified with SEM seat shocks, there was still a need to deliver the correct deceleration pulse to the Bogie test platform. The need for controlling the crash pulse was a perfect application for an SEM impact barrier (Fig. 6). While past SEM impact barrier tests never tried to deliver such a tailored crash pulse, the Principal Investigator was confident that by stacking multiple shock housings, and altering the ejection materials' properties, that a spec 8-g max by 250 ms triangular crash pulse could be achieved. By including another shock function in the HSR-45 study, essentially two systems could be tested for the price of one, plus these two applications would help convey the wide range of impact load performance that the SEM technology could deliver; from seat shocks loads in the hundreds of lbs_f of restraint load, up to impact barrier loads in the tens of thousands of lbs_f and even higher for some other rail and ship crash load applications.

The SEM impact barrier was used in nine full-scale impact tests and one static load test. The two pieces of hardware that were reused in all nine of the impact tests, with no repairs or modifications, were the mobile impact sled with its diagonal stiffening beams, and the



Fig. 6

ground mounted I-beam assembly. The forward white rubber bumping pad was set on the front of the vertical 4.0” x 4.0” x 0.25” steel post, to reduce the spike loading at initial Bogie vehicle contact. The two visible bolts under the #7 label, in Fig. 6, are the attach bolts between the impact sled and the SEM piston assembly. The SEM piston assembly slides inside the two visible SEM shock housings and is structurally accessed through the 0.375” ejection groove. Note: Two other SEM shock housings are on the far side of the I-beam assembly. Therefore, the barrier’s SEM shock housing sets consisted of four separate SEM shock housings and two separate SEM impact piston assemblies. The four shock housings were then filled with 1.0” OD elastomer cord of varying durometers and with various types of fiber wraps. The only parts that were replaced between tests were the spent SEM shock housings. The removal and replacement of the spent SEM shock housings was quite expedient. After learning the general hardware setup from the first rework, a two or three person TTI team could replace the spent SEM housings with a new housing set in about 10 minutes.

The impact sled and the I-beam mount were not the only barrier components reused. In the initial 2004 TTI/SEM test effort the impact barrier’s shock housings were considered to be expendable, which was partially due to the projected rework time, although, after the first test effort there was no discernable yielding of the shock housings. Therefore, for the 2005 tests, two of the SEM housing sets were reused by reloading new shock cord in the used SEM shock housing assemblies. Those reworked housing assemblies were used in test runs 8 and 9 and there was no notable shift in the system performance.

While past SEM impact barrier tests had been conducted, none of those barriers had such a wide performance requirement (the triangular crash pulse). Therefore, the HSR-45 Technical Panel suggested that static testing be conducted on the completed impact barrier assembly before running the impact tests at TTI. To run the static test the I-beam assembly was slightly modified to receive two 4.0” ID hydraulic actuators with 24.0” of available stroke (Fig. 7), and a spacer was added to supply the remaining 24.0” of travel. The actuators had to be displaced twice since the spec triangular deceleration pulse would result in a travel distance of 48.0”. The spec



Fig. 7

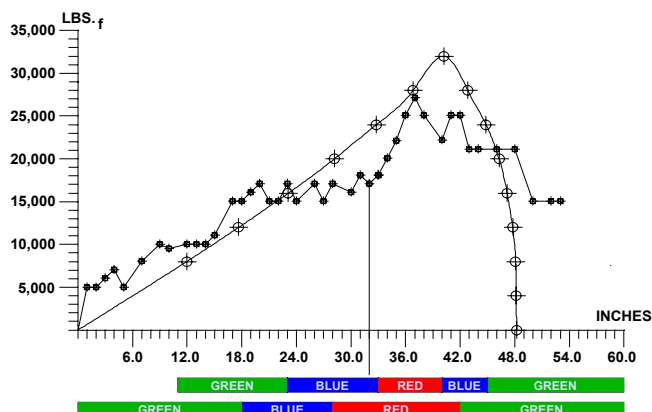


Fig. 8

triangular crash pulse formula went through a double integration to obtain the various travel distances at which certain loads would be needed. The smooth line plot of Fig. 8 gives the deceleration load at various x-locations or stations that the 4,000 lbs Bogie vehicle would require, to achieve the spec deceleration pulse. The jagged plot gives the actual restraint loads measured. The bar at the base of the graph shows the loading of the 3 durometers of ejection material or rubber cord, green is Low Density (LD) 50-D; blue is Medium Density (MD) 60-D; red is High Density (HD) 70-D. Note: Durometer (D) is a measure of a materials hardness or ductility and, depending on the material type, there are five different methods to measure a material's hardness (12) (e.g. Brinell Hardness for metals, Rockwell M & Rockwell R for plastics, Durometer D & Durometer A for elastomers). The static test proved the max-spec load could not be achieved without some modifications to the ejection material (e.g. stiffer durometer and/or different fiber wrap). Note: Fiber wrap was a general term used for the addition of an outside layer/s of high strength glass fiber tape and/or a higher strength carbon fiber tape, to the various durometers of rubber cord. Also, to get a better load match between the spec and actual performance curves, the static test curve needed to be shifted to the left or up station or to the front of the impact barrier (e.g. note in Fig. 8 the vertical line needs to move to the left to obtain a better match between the curves). Both of these design shifts were made, those being a change in the fiber wrap and a forward station shift of the stiffer ejection material load. These changes resulted in the final impact barrier load shown in Fig. 9, which was used in all of the seat test runs. The only fiber tape change was on the HD-GT slug (e.g. High Density – Graphite Tape), where the normal six alternating layers of glass fiber tape, which had a 300 lbs/in break strength, were replaced with one layer of carbon fiber tape with a 3,000 lbs/in break strength and two glass fiber tape layers.

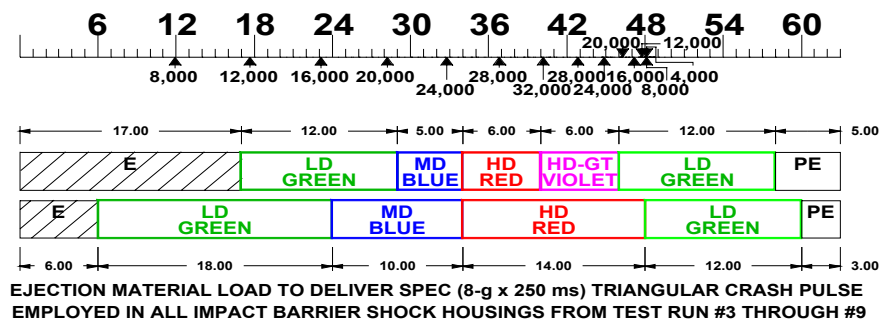


Fig. 9

While not perfect, this particular SEM barrier design came very close to delivering the spec 8-g by 250 ms triangular crash pulse for the majority of the test runs (Figs. 10.1 – 10.9 show all of the g-load performance plots from all nine impact tests). A single accelerometer was placed on the floor plate of the Bogie vehicle and Line Plot #2 or the jagged performance line shows the actual g-load history experienced by the Bogie vehicle assembly. The initial two load spikes that are present in all of the plots are due to initial impact events. The initial contact between the Bogie and impact sled created the first load spike, the sled then bounced or accelerated forward to where the Bogie and sled were once again separated. The second load spike on Line Plot #2 came from the re-contact of the Bogie vehicle with the impact sled when the Bogie caught up with the sled a second time. Line Plot #1 or the straight line triangular graph on all nine plots shows the spec 8-g by 250 ms triangular crash pulse. While the actual performance plots are not an exact match to the spec triangular plot, they are surprisingly close to the desired spec performance, especially when compared to some of the full-scale rail impact tests, such as those in Fig. 3. Of course the full-scale rail car tests are much more complex systems undergoing buckling and crushing, so they are more difficult to control.

For comparison purposes, it is notable that the performance plots keep getting closer and closer to the spec triangular crash pulse, as the tests progress. The first two performance plots (Figs. 10.1 & 10.2) represent a low- and a high-impact barrier performance respectively. The third test (Fig. 10.3) represents the ideal ejection material load per Fig. 9, which was unaltered in the remaining six tests. One of the reasons the 3rd performance plot did not provide an ideal match with the spec triangular crash pulse is due to the absence of any secondary impacts from the unbelted test dummies. The Bogie was ballasted in the first three tests to approximately the same weight of a Bogie with test seats and test dummies. Those ballast plates were immobile, so there were no secondary impacts to influence the Bogie's deceleration pulse. While there were little discernable displacements of the SEM seat shocks in the 4th through 6th tests (Figs. 10.4 thru 10.6) the dummy dynamics and the yielding passenger seats did give a more accurate alignment between the actual and spec deceleration pulses. Finally, the 7th through 9th tests (Figs. 10.7 thru 10.9) had the dummy and seat dynamics, plus the added displacement characteristics of the SEM seat shocks. With the added seat shock dynamics the actual deceleration plot came even closer to an ideal spec match, especially in the 9th test run (Fig. 10.9). Such an ideal performance was by no means modeled or designed into the SEM impact barrier, so it occurred with a little bit of luck. This performance difference helps show the contribution of the dummy and seat dynamics to the overall vehicle dynamics of the 4,100 lbs Bogie assembly (e.g. extra 100 lbs includes instrumentation).

Lastly, there were a couple of changes in the test parameters. One was an increase in the impact velocity for all of the tests. The spec impact velocity was 21.9 mph but it was increased to 23.5 mph to make up for the barrier's sled weight. To achieve a final 21.9 mph for the 4,100 lbs Bogie and 300 lbs sled combination, conservation of momentum required the 4,100 lbs vehicle to have an initial impact velocity of 23.5 mph. The other change to the SEM impact barrier was the addition of 6.0" of free travel, with the intent of equalizing the Bogie/sled velocity. This 6.0" of travel was removed in the last three tests (Test Run #7 through #9). Therefore, that 6.0" should be removed from the total travel distance of the first six tests (Test Run #1 through #6). The ideal spec travel for the Bogie/sled should be 48.0". The following list gives the SEM barrier performance for the various tests.

- Test Run #1** - Ballasted Bogie test using the lowest restraint load performance SEM impact barrier. The Bogie vehicle impacted the barrier at a speed of 23.45 mph and the sled traveled a total distance of 57.5" or 51.5" with the 6.0" of free travel removed.
- Test Run #2** - Ballasted Bogie test using the highest restraint load performance SEM impact barrier. The Bogie vehicle impacted the barrier at a speed of 24.33 mph and the sled traveled a total distance of 44.1" or 38.1" with the 6.0" of free travel removed.
- Test Run #3** - Ballasted Bogie test providing the spec 8-g x 250 ms restraint load performance. The Bogie vehicle impacted the barrier at a speed of 23.98 mph and the sled traveled a total distance of 48.9" or 42.9" with the 6.0" of free travel removed.
- Test Run #4** - Full scale seat test using #3 barrier load. The Bogie vehicle impacted the barrier at a speed of 23.64 mph and the impact sled traveled a total distance of 48.2" or 42.2" with the 6.0" of free travel removed.
- Test Run #5** - Full scale seat test using #3 barrier load. The Bogie vehicle impacted the barrier at a speed of 23.81 mph and the impact sled traveled a total distance of 43.7" or 37.7" with the 6.0" of free travel removed. Note: The forward seat failed due to incorrect bolt attachment, thus giving a smaller travel distance.
- Test Run #6** - Full scale seat test using #3 barrier load. The Bogie vehicle impacted the barrier at a speed of 23.83 mph and the impact sled traveled a total distance of 48.6" or 42.6" with the 6.0" of free travel removed.
- Test Run #7** - 2005 extension, full scale seat test using #3 barrier load. The Bogie vehicle impacted the barrier at a speed of 23.24 mph and the impact sled traveled a total distance of 41.4".
- Test Run #8** - 2005 extension, full scale seat test using #3 barrier load. The Bogie vehicle impacted the barrier at a speed of 23.18 mph and the impact sled traveled a total distance of 43.07".
- Test Run #9** - 2005 extension, full scale seat test using #3 barrier load. The Bogie vehicle impacted the barrier at a speed of 23.11 mph and the impact sled traveled a total distance of 39.37".

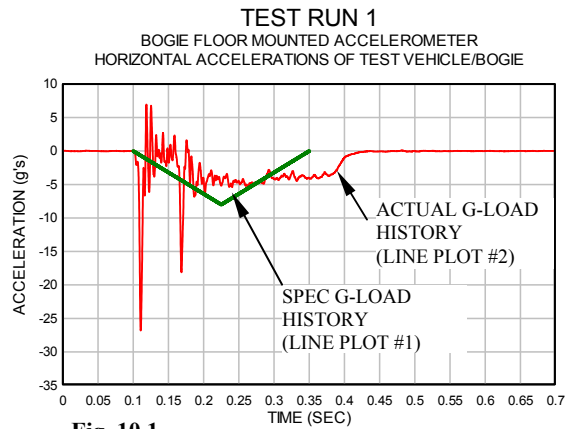


Fig. 10.1

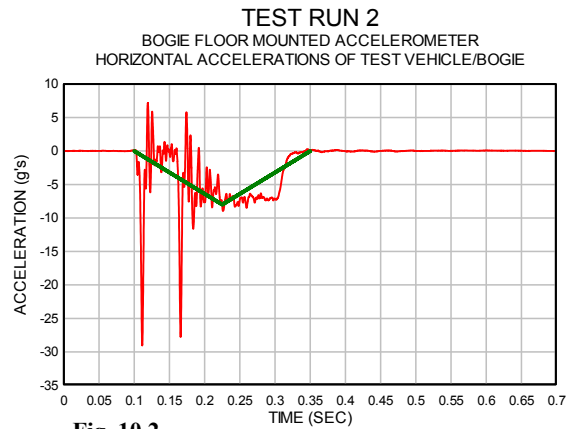


Fig. 10.2

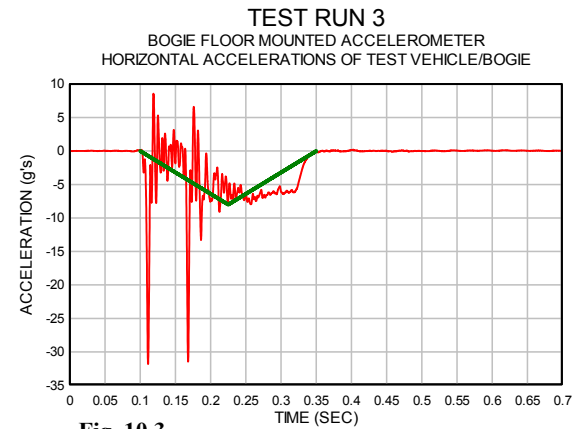


Fig. 10.3

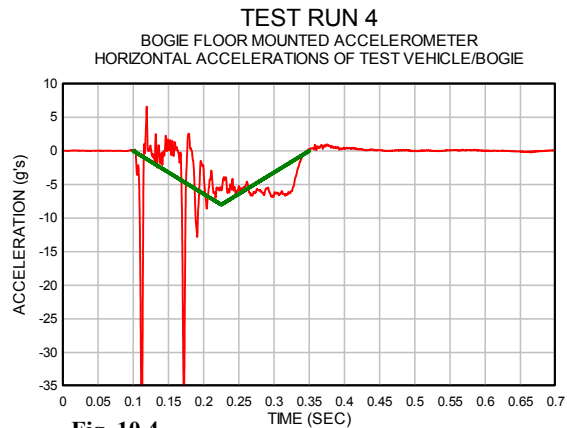


Fig. 10.4

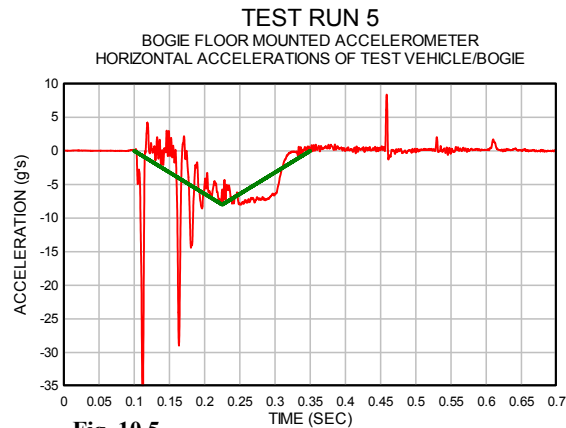


Fig. 10.5

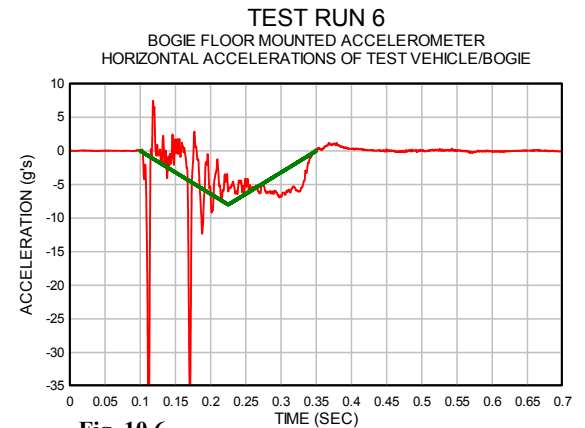


Fig. 10.6

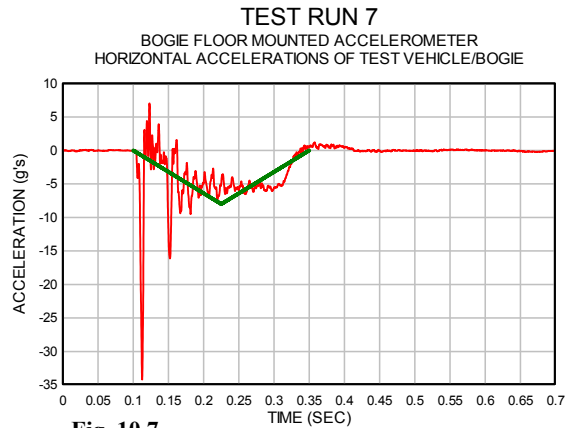


Fig. 10.7

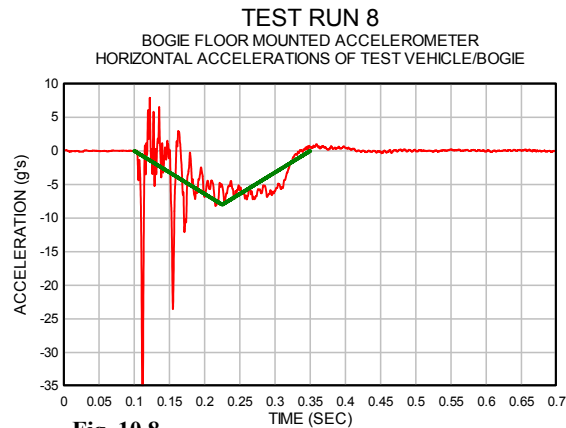


Fig. 10.8

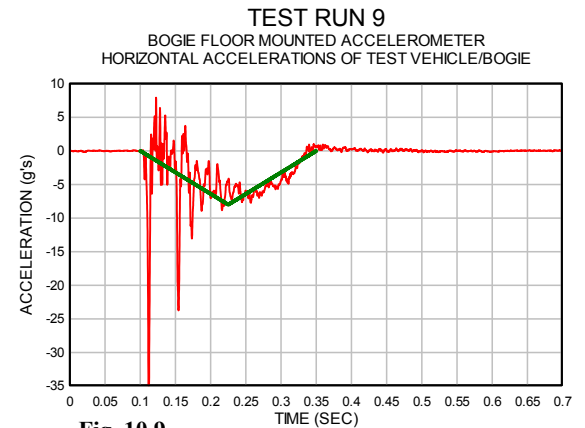


Fig. 10.9

Stress Modeling of Test Hardware:

Finite Element Modeling (FEM) was performed on the two main test hardware structures, i.e., the Bogie vehicle and the SEM impact barrier. By doing this, it was determined that none of the critical structures would fail and/or be damaged, even if the Bogie and barrier assemblies went through multiple impact tests. The results indicated very few high stress areas on either structure; most of the structures modeled were in the low stress zone, so that few of the structures or individual parts would experience any notable yielding.

Instead of doing a detailed FEM model of the two seat shock structures, the design of the SEM seat shocks were spun off from existing seat attachment hardware, such as the mounting brackets and the size and placement of the attachment bolts. The main premise being that the catastrophic failure loads should be reduced with the use of the SEM seat shocks; plus if the SEM seat shocks used more substantial structures and parts than the existing part designs, the potential for seat breakaway should be eliminated. This did prove to be the case with all of the seat shocks tested, except the 5th seat test where the bolt attachments for the floor shock failed. This was due to an inadequate number of threads being engaged on the attachment bolts and not due to structural failure of any of the floor shock or seat parts.

The need for modeling the seat hardware undergoing impact loading became redundant after the completion of the first TTI/SEM test effort, since all of the x-loading and bending moments were ascertained from the seat load cells in test runs #4 and #6.

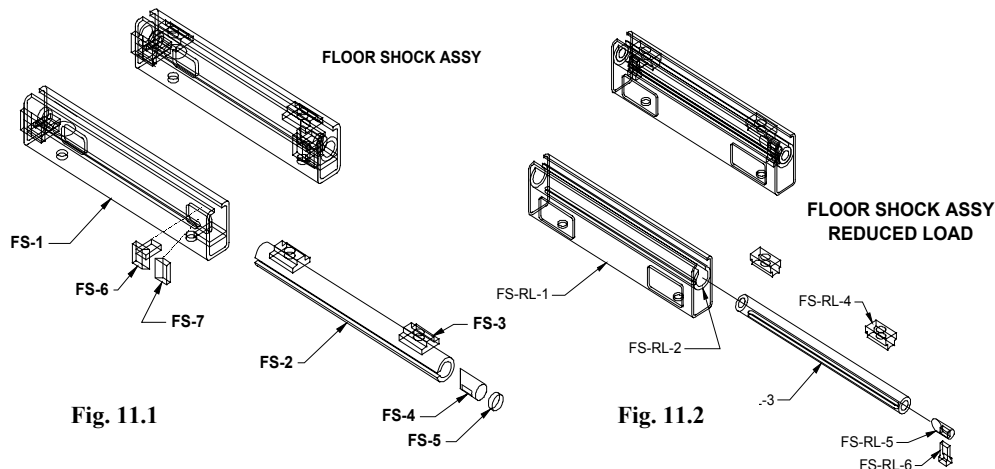
Flow modeling of the ejection material would have been a valuable exercise but since the computer model would have had to take into account a dynamic and not a static load model, it proved to be too difficult to model with the available FEM software.

Design, Fabrication and Static Testing of SEM Seat Shocks:

From the start there were two basic design types for the SEM seat shock to interface with the two attachment points for the stock three-passenger seat. This particular seat model had two different attach points; a window side attach point where the seat is mounted to the adjoining wall and the second attach point was with the floor, between the aisle-seated and middle-seated passengers. The location of these two attach points altered the performance requirements for the two SEM shock types; the wall model had lower longitudinal loading since it was essentially being impacted by only one of the test dummies. The bending moments for the wall attachment were lower since the attach point was nearer to the impact point center. The floor shock experienced higher loading due to the impact of essentially two test dummies, plus the bending moment was greater due to the longer moment arm between the floor and impact point center. The following discussion is a summary of the design progression of both SEM seat shock models.

Floor Shock #1 - The 1st model (Fig. 11.1) used a 0.75" ID shock housing and this housing was in direct contact with the outer rectangular sleeve. This was the floor shock model used in test runs #4 through #6, and due to its high SEM restraint load performance and frictional losses, there was very little displacement.

Floor Shock #2 - The 2nd floor shock tested (Fig. 11.2) downsized the shock housing to a 0.5" OD and put the inner housing in a protective circular sleeve. Also, the inner housing received a Teflon coat to reduce the overall frictional losses. This model went through a series of static tests but it failed due to the high bending moment loads; these loads were administered in the second static test effort.



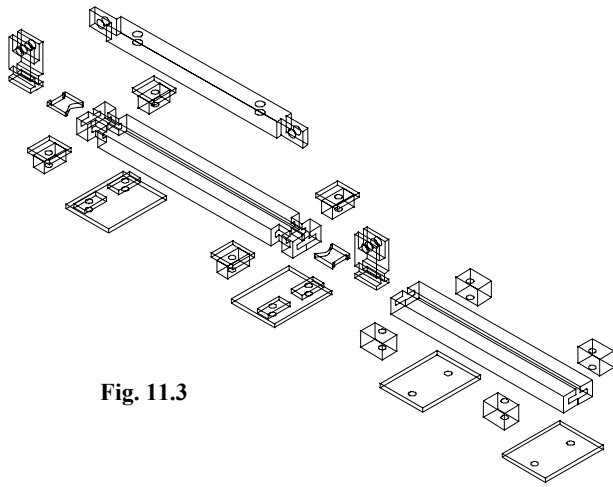


Fig. 11.3

Floor Shock #3 - The 3rd floor shock model (Fig. 11.3) replaced the circular housing cross-section with a rectangular cross-section. The purpose of this design change was to survive the high bending moments that were being delivered to the floor shock (often exceeding 7,000 ft-lbs), while reducing the friction enough to still deliver the lower restraint loads (e.g. x-loading in the range of 600 lbs). This design was used in test runs #7 through #9.

Wall Shock #1 - The 1st wall shock (Fig. 12.1) had a 0.5" ID but it used some higher durometer 0.5" rubber cord. Also, there was no type of lubrication added between the inner and outer housings. Therefore, this wall model experienced very little displacement, except in the 5th test due to the extra loading from the breakaway of the floor shock. This model was used in test runs #4 through #6.

Wall Shock #2 - The 2nd wall shock model (Fig. 12.2) had no change to the ID but the ejection groove width was slightly increased. Also, a Teflon coating was added to the inner shock housing, to reduce the frictional losses. Lastly a lower

durometer ejection material was used in all of the last three tests (test runs #7 through #9). These design changes delivered a lower restraint load performance, thereby allowing for some substantial displacements.

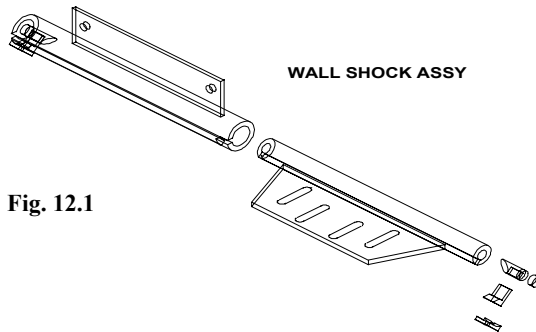


Fig. 12.1

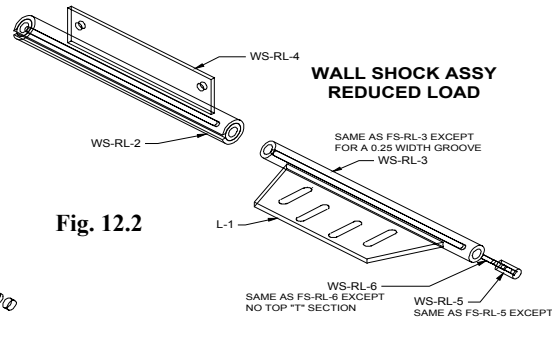


Fig. 12.2

Both types of SEM seat shock models (Figs. 15.1 and 16.1) went through design changes to reduce their load performance to approximately 1/3 of the original load performance. While the above sketches (Figs. 15.1 through 16.2) give a more detailed breakdown of the design changes that were made, some of the more general points should be touched upon. In general the floor shock model went through three complete redesigns and the wall shock model went through two lesser design upgrades. Also, the final floor and wall shock models went through a more aggressive series of static load tests, where large bending moments were delivered to the test hardware. This was achieved by adding a substantial cantilever beam structure (Fig. 13.2) to the existing static load test tool (Fig. 13.1). These large bending moment tests eliminated the use of the 2nd floor shock design (Fig. 11.2) in the full scale 2005 TTI/SEM seat test. Undoubtedly that particular model would have pulled apart under the full-scale impact testing at TTI.

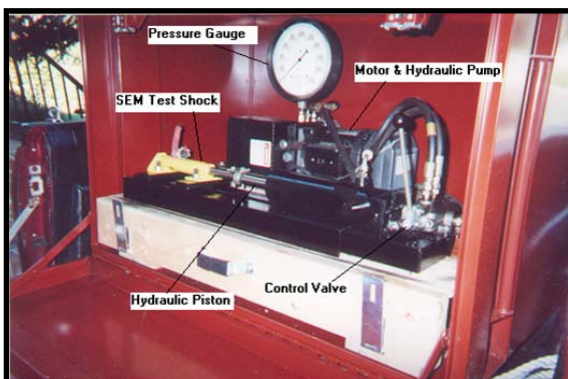


Fig. 13.1



Fig. 13.2

Both shock models were designed to take comparable impact loads both in the forward and reverse directions. The reason for this feature was due to the mounting directions for the typical railcar seat, where it could be mounted in a forward facing or rearward facing direction. Also, the typical passenger car can experience equivalent crash loading in both travel directions, from a train being rear-

ended or from a moving train hitting a forward structure/vehicle. All of the SEM seat shock designs included this feature of being able to supply the same load and the same travel in both directions. Some of the valuable data that came from the first TTI/SEM test series that were run in 2004 was the actual seat loads, both horizontal *and* vertical, that were being delivered to the SEM seat shocks. The vertical load cells that were shown in Fig. 5 provided some of the vertical load data for both the floor and wall shocks. This load data was used in the design of the cantilever load beam of Fig. 13.2 and it allowed for some substantial bending moments, especially for the floor shock, to be delivered to the new shock models. It should also be pointed out that these vertical load readings were typical for all of the seat tests.

Because the vertical load cell spacing was very close to 1.0 ft, the vertical load values were very close to the bending moment values. Therefore, the floor shocks needed to be able to displace with an approximate bending moment of 7,000 ft-lbs and the wall shock had to function under a much lower bending moment of 1,000 ft-lbs. Having the structures survive the bending moments actually was not that difficult, since the original SEM seat shock designs survived these loads, but they had no shock function and/or displacement. The goal was to supply a relatively low restraint load performance while experiencing these high moment loads. For instance, the wall shock had to deliver an approximate 300 lbs_f restraint load while experiencing a 1,000 ft-lbs torque, a nearly 3 to 1 ratio. The floor shock performance was even more aggressive since it had to provide an approximate 600 lbs_f restraint load while experiencing a 7,000 ft-lbs torque, a severe 11 to 1 ratio. While not impossible, it was difficult to achieve since the sliding friction loads of the parts needed to be greatly reduced, otherwise the frictional loading would interfere with the SEM restraint loading. For instance, if a relatively low friction coefficient of 0.1 was assumed then the 7,000 lbs vertical load would add **700 lbs** to the SEM restraint load value of 600 lbs. As previously mentioned, the friction coefficients were reduced with the addition of a Teflon coating for the wall shock model, but the 3rd floor shock model used two thin layers of HDPE sheet on the down station slide piston. The HDPE sheets had a binding problem in the 8th test run, which greatly altered the performance. Both of the plastic layers were also lubricated with a silicone grease, with the intent to reduce the friction load contribution to a minimum. While not being able to quantify the frictional load contribution for each shock type, the static load tests were able to quantify the load performance of both the wall and floor shock models, to ensure they were in the desired performance range.

Test Results from Seat Impact Tests Conducted at TTI in Nov. 2004 and Nov. 2005:

On November 10-12, 2004 six impact tests were run at TTI test facilities in College Station, TX, with the intent of collecting crash data on a production model - passenger railcar seat modified with SEM seat shocks. A total of six impact tests were run and the last three tests used all of the test hardware shown in Fig. 14.1, those being, the Bogie test vehicle; the SEM impact barrier; the two production model passenger seats; the three test dummies, one of which was instrumented; one wall and one floor SEM seat shock mounted under the forward seat; and a TTI tow truck with tow cable, pulley assembly and side guide cable (not shown), to give the Bogie assembly a controlled pull into the impact barrier at an adjusted 23.5 mph impact velocity. The first three impact tests were run to test the load

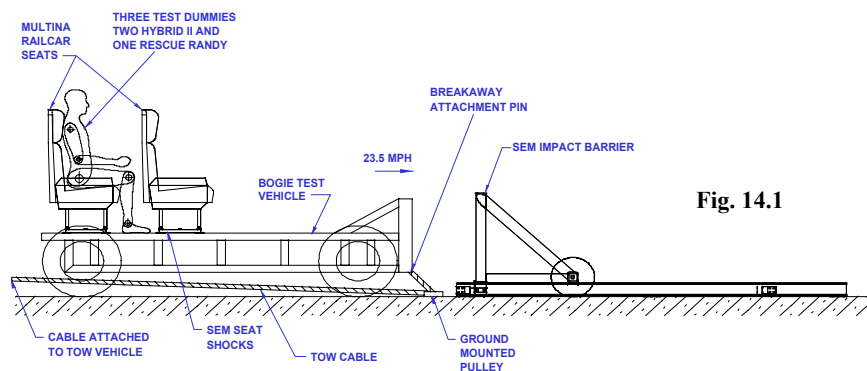


Fig. 14.1

performance of the SEM impact barrier, so that it could be tailored to deliver a spec 8-g x 250 ms triangular crash pulse. In the first three tests the seats and test dummies were replaced with ballast plates of comparable weight. The first three impact tests allowed for the TTI test team to get some experience with the new Bogie test platform, before running the seat tests.

The overall test setup came very close to delivering the desired triangular crash pulse to the Bogie assembly, as shown in Fig. 14.2 (this picture is the tail-end of the impact event from the 6th test). While not an exact match with the spec crash loads, all of the test runs came very close to exposing the shock modified seats to a real-world crash load environment.



Fig. 14.2

expectation, based on past test reports, that higher crash loads would be delivered to the SEM seat shocks. Because of this the first SEM seat shock models were designed to displace under much higher loads.

The original design of the set shocks was based, in part, on crash test data using old seat designs; some of which broke away during spec crash loading (6). The seats used in this project were more modern and, as a result, the newer seat structures did all of the yielding and energy absorption, so the seat shocks experienced very little displacement due to their higher restraint load performance.

While this was a seeming set back, some valuable data was obtained in terms of the crash load performance of the stock passenger seats, which were exposed to a standard impact pulse that was delivered by the SEM barrier in all six seat tests. Since the SEM shocks did not displace in the Nov. 04 test effort, the crash load history on the seats and the instrumented test dummy provided very useful baseline data for a seat that had not been shock modified. This proved to be very useful since it provided a comparison of the crash load data for a stock and an SEM shock modified seat.

Since the first TTI/SEM test effort didn't provide any data for a railcar seat that had been SEM shock modified, the High-Speed Rail IDEA Committee agreed to an extension to the HSR-45 study. This extension provided the funding to run three more crash tests, with redesigned SEM seat shocks. These shocks were modified and static tested to deliver a lower restraint load performance. On November 21-22, 2005 another three impact tests were run at TTI's test facilities. This time the redesigned, low-load SEM seat shocks were employed. The only other change to the overall test setup was the removal of the 6.0" of free travel that was part of the original SEM barrier's ejection material load, which was used in all of the first six tests. There were substantial displacements of the SEM seat shocks in the second test effort. This gave some good comparative data between the first test run, with its essentially non-shock-modified test seats, and the same seats that had been shock modified in the Nov. 2005 test effort. The data between the two test efforts correlates well. The following discussion of test results compares the test data and photos for the Nov. 2004 and Nov. 2005 test efforts.

Test Run #4 (November 2004):

Test Run #4 used the first complete Bogie setup, with test seats, test dummies, seat load cells and the SEM seat shocks. This test was run after completing the first three impact tests with the ballasted Bogie. The collision environment for this test came very close to meeting the spec collision environment with a 23.64 mph impact speed and a 7-g peak deceleration (Fig. 10.4, pg. 18). As previously mentioned, the seat shocks in this test were too stiff to have any displacement, therefore the passenger seat did all of the yielding and energy absorption. The HIC_{36ms} value of 981.7 (Fig. 21.1 and Fig. 21.2 for the HIC_{15ms} value, pg. 29) was within the max spec value of $HIC_{36ms} = 1,000$. The chest accelerations were very low with a max spike acceleration of only 23-g's, whereas the spec required that a max value of 60-g's over 3 ms not be exceeded. This was the only test where the chest acceleration measurements were obtained, as the seat breakaway in Test Run #5 resulted in damage to the chest accelerometers. This was not considered a big issue, since the initial measurements were so low. Another interesting result was the very low femur loads of only 800 lbs per femur (Fig. 23.1 and 23.2, pg. 31), versus the spec requirement of 2,250 lbs. This was interesting because the femur load data from the 1996 DOT/FRA tests ranged in the 2,000 lbs to 3,000 lbs (Table 4, pg. 12), and the one seat that didn't fail in the 1999 DOT/FRA test (Table 3, pg. 12) also had a max femur load of over 3,000 lbs. Note: At the time of HSR-45 tests neither of the previous seat tests were an exact match in terms of seat construction (e.g. heavier and stiffer older model seat) (6) which of course was designed before the APTA SS-C&S-016-99 spec release; plus there were greater seat separations (pitch) of 41 and 52 inches versus the 33 inches used in the HSR-45 study (6); and lastly the seat that didn't fail in the 1999 DOT/FRA test was reinforced to prevent this failure, so once again the crash load performance for this particular seat was not representative of a production model. For a better comparison of SEM modified seating and unmodified M-Style seating, a check of a July 2002 Volpe seat test would be useful (14). The lower femur loads were consistent with all of the stock 3-passenger seats, whether this model seat was shock isolated or not. While there was no displacement of the seat shocks, there was valuable load data obtained for the seat, in terms of its x and y loading (Fig. 24.1 wall shock x-loading, Fig. 24.2 floor shock x-loading). This information allowed the setting of the shock load performance in the second test series which was run in Nov. 2005. Lastly, the general containment of the test dummies in Test Run #4 was actually quite good (Fig. 21.1, pg. 29) since all of the dummies stayed on the test vehicle and essentially were contained behind the front seat.

Test Run #5 (November 2004):

Test Run #5 was the only seat test where the front seat failed by breaking free of the floor attachment (Fig 21.2, pg. 29). This failure had nothing to do with a failure of the seat structures or SEM floor shock structures, but instead was due to the incorrect bolt length being used, between the floor shock and the seat's pedestal structure. This was due to some spacer plates being added without increasing the bolt length. While all of the load data from the test dummy and the front seat's load cell were essentially unusable, some valuable data was still obtained from this test. This was the only test where some nominal displacement of the wall shock was obtained (1.4"). This was due to the extra loading being delivered to the wall shock because of the floor shock's detachment. Also, the overall Bogie deceleration hit the spec 8-g max value again (Fig. 10.5, pg. 18), so this showed that the dummy dynamics was a large enough influence on the overall crash dynamics of the Bogie assembly. As mentioned, the seat breakaway tests resulted in damage to the dummy chest accelerometers.

Test Run #6 (November 2004):

As with Test Run #4, Test Run #6 had very little displacement of the seat shocks. The original floor shock model did have about 0.5" of travel (Fig. 15.1) but the original wall shock model had no notable movement (Fig. 15.2). The SEM impact barrier had close to the same performance (Fig. 10.6) as the barrier in the 4th test but for some reason the HIC_{36ms} values had a substantial increase to 1,314.3. It is unknown why the HIC values increased by so much, since the only known difference was a slight increase in the impact speed (e.g. 23.64

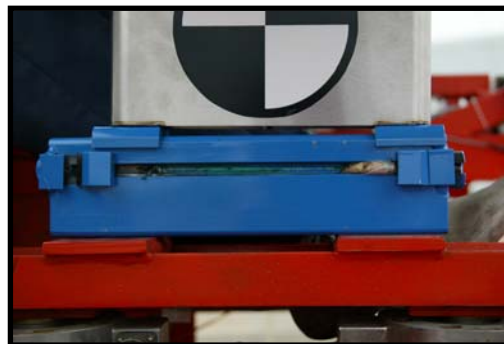


Fig. 15.1

mph in 4th test, up to 23.83 mph in the 6th test) and the slight displacement in the floor shock. The only other interesting difference in this test was the right femur load reading (Fig. 23.6, pg. 31), which was 1,150 lbs. This was the highest femur load reading. The next highest was 900 lbs from the 8th test run.

Test Run #7 (November 2005):

Test Run #7 was the first test run in the Nov. 2005 test series and it used the substantially redesigned SEM floor shock (Fig. 16) and the slightly upgraded SEM wall shock. The impact speed for this test was 23.24 mph and the Bogie assembly experienced a peak g-load of approximately 7-g's (Fig. 10.7, pg. 18). The redesigned seat shocks had some substantial displacements; the floor shock had an 8.0" displacement and the wall shock had a 5.0" displacement. Even with these substantial displacements there was no notable improvement in the Human Injury Limits (Table 2, pg. 11). The HIC_{36ms} value of 1039.0 was slightly above the spec value and there was no notable change in the femur loading, since both left and right peak load values were 800 lbs (Figs. 23.7 and 23.8). The only notable change was in the loading behavior of the floor shock (Fig. 24.8). The load history of the floor shock for Test Runs #7 through #9 (Figs. 24.8, 24.10, 24.12) had two notable load spikes, whereas Test Run #4 and #6 (Figs. 24.2 and 24.6) had a single load pulse. While the actual mechanics for this alternate load history is unknown, it is assumed that the forward movement of the two SEM seat shocks allowed for a secondary impact of some part of the test dummies' anatomy. There was no such dual load spike behavior for any of the newer wall shock models (Figs. 24.7, 24.9, 24.11). A more detailed hypothesis as to the reason for this alternate load history will be presented in Test Summary section.

Test Run #8 (November 2005):

Test Run #8 had a number of unique behaviors much like Test Run # 5. It had the lowest HIC_{36ms} value of any of the tests, 408.6. It is not known if that was due to the SEM seat shocks' function or the failure of the seat back structure (Fig. 17), right where the middle instrumented test dummy made contact. It is assumed that this "punch through" of the center seat back and near the top of the seat (Fig. 17) could possibly contribute to a substantial reduction in the HIC values. But the question that arises is why did this seat back fail under these particular test parameters? Could it have had anything to do with the load history of this particular seat shock? The interesting thing about Test Run #8's SEM seat shocks was they actually employed a softer or lower durometer ejection material (e.g. 20-D) than the durometer used in the 7th test (e.g.30-D). Even with the lower durometer ejection material, the 8th test shocks had less displacement. The wall shock displaced 2.75" and the floor shock displaced 5.5". The reason for the lower displacement was due to the binding of the floor shock, where the two HDPE plastic sheets were not set back far enough to where the lower surface of the floor shock's forward skid had total contact. Despite this, there was still little variation in the femur loading. The right femur load increase to about 900 lbs from the more consistent 800 lbs. So again this may show the initial load dynamics may have more influence over the test dummy's Human Injury Limits than the later dynamics of the seat structures or seat shocks.

Test Run #9 (November 2005):

Test Run #9 used the lowest durometer ejection material (e.g. 10-D). Also, the HDPE sheets were setup properly in the floor shock for this test run. Therefore the 9th test had the greatest displacements. The floor shock went through 9.0" of travel, which neared its max available travel of 10.0" (Fig. 18.1). But the wall shock actually did bottom out (Figs. 23.2 and 23.3 next page), to where the inner housing went through some



Fig. 15.2



Fig. 16



Fig. 17



Fig. 18.1



Fig. 18.2

notable yielding. The interesting thing about this test setup was the higher than normal loading on the horizontal load cells, once both of the shocks bottomed out. The initial impact loading was slightly lower than normal, for most of the travel, but when the wall shock bottomed out, it experienced a load spike that peaked at 2,000 lbs. This compares to a normal restraint load of about 1,000 lbs to 1,100 lbs. The floor shock experienced a peak loading of 3,000 lbs, whereas it normally supplied a restraint load that ranged from 1,700 lbs to 1,800 lbs. Although, even with these late-stage peak loads, the general injury levels for the test dummy were essentially unchanged. For instance, the HIC_{36ms} value was 1005.0; and while some of the lowest femur loads were experienced (e.g. 650 lbs for the left femur and 750 lbs for the right femur) these loads were close to the other test values. So again the question arises, why doesn't a reduction in the late-stage load environment have more of an influence on the Human Injury Limits? From the test data, it appears that if the late-stage load environment (the majority of the time after initial dummy contact) is *reduced* from the use of SEM seat shocks, there is little affect; or if the late stage load environment is *increased* due to an abrupt stop at the end of the seat shock travel; neither action appeared to have a great deal of influence over the Human Injury Limits.



Fig. 18.3

Test Summary:

The following table gives a summary of the TTI/SEM crash test data, from Test Runs 4 through 9 and while not an ideal match between Table 3 and 4 due to test sample variation (e.g. stiffer and older seat models) and test parameter variations (e.g. seat separation, impact speeds); the test data is still in the “ballpark” and is reasonably good for comparison purposes and still holds some level of comparable railcar seat test data. It should be noted that both of these earlier tests efforts used older seat models, plus one of the test efforts (Table 3) used higher impact speeds (e.g. 35 mph instead of 23.5 mph) and the Table 3 test effort used a much more complex crash test platform (e.g. full sized passenger railcar structure undergoing buckling instead of a Bogie vehicle & SEM barrier combination). Also note, the test results of Table 4 had a much closer spec crash environment but most of their test seats failed, which most likely means that max test dummy loading was probably not achieved.

Table 5

Select Data from HSR-45 TTI/SEM Seat Tests Nov. 2004 & Nov. 2005

Seat Test #	Impact Speed mph	Peak Bogie g's	HIC _{36ms}	HIC _{15ms}	Chest (g's)	Max Femur Load Left (lbs)	Max Femur Load Right (lbs)	Wall Shock Max X-load (lbs)	Floor Shock Max X-load (lbs)	Wall Shock Travel (in)	Floor Shock Travel (in)	Ejection Material Durometer
#4	23.64	7-g's	981.7	981.7	23	800	800	1000	1800	0.0	0.0	70-D
#5 (Failed)	23.81	8-g's	604.5	352.3	N/A	700	500	1200	1500	1.4	0.0	60-D
#6	23.83	7-g's	1314.3	915.0	N/A	800	1150	1100	1700	0.0	0.5	50-D
#7	23.24	7-g's	1039.0	670.3	N/A	800	800	1000	1800	5.0	8.0	30-D
#8	23.18	8-g's	408.6	408.6	N/A	800	900	1000	1700	2.75	5.5	20-D
#9	23.11	8-g's	1005.0	466.5	N/A	650	750	2000	3000	8.75	9.0	10-D

While the overall test data for the HSR-45 study were reasonably quantified in terms of the actual accelerometer and load cell readings, there were some interesting performance numbers or behavior which needed some additional review. As touched upon previously, there were some changes in the horizontal loading or x-loading of the floor shocks. For instance, in the first test series (Figs. 24.2, 24.6, Note: Floor shock in Fig. 24.4 broke free) the floor shocks' x-loading was a single and relatively constant pulse; whereas the floor shocks in the second crash test series (Figs. 24.8, 24.10, 24.12) had two distinct pulse loads. Compare this now to all of the wall shock performances (Figs. 24.1, 24.3, 24.5, 24.7, 24.9, 24.11) where the loading was essentially a single pulse load for the majority of the load histories (Note: There was a short dip in the load performance of Fig. 24.3 at about 0.33 sec). There are also two other considerations, the first being the breakaway of the floor shock attachment in the 5th test run (Figs. 24.3 & 24.4) and the second being that the seat shocks in the first three test series (test #4 - #6 and Figs. 24.1-24.6) had little if any displacement, but there was ample displacement of both seat shock models in the last three tests (test #7 - #9, Table 5).

From the available data there were a couple of theories as to why only the floor shocks in the second test effort (Nov. 05) exhibited a double crash pulse, whereas the wall shocks in all six of the seat tests, in both test efforts (Nov 04 & Nov. 05) had a similar single pulse load behavior. The first theory for this behavior came from a review of some of the earlier test photos. A series of high speed photos was taken in the first TTI/SEM test effort. These photos were taken on both sides of the point of impact, between Bogie and barrier, as well as from an overhead camera (Figs. 24.1 – 24.4). The overhead photos show a sequence of photos from the 6th test, which were taken shortly after all of the dummies' upper torsos had started to impact the forward seat (Fig. 19.1). Note: The driver's side of the Bogie vehicle is on the bottom of the photo and this is the side which had the wall-mounted SEM seat shock. The attach point for the SEM floor shock is mounted between the middle test dummy and passenger side test dummy or the two dummies in the light color shirts (Fig. 19.1). (Bogie vehicle is moving right to left.)

The following sequence of photos shows the test dummies at initial head contact (Fig. 19.1); the next photo (Fig. 19.2) catches a view of the near maximum displacement of the seat back, with both elastic and permanent yielding being viewed; the next photo (Fig. 19.3) shows the position of the test dummies at just about the point they bounce back and start losing contact with the forward seat structure; and the final photo (Fig. 19.4) shows the different rate of recoil of the three test dummies as they fall back into the rear seat. An interesting behavior was noted in the second photo (Fig. 19.2) which could possibly help explain the difference in pulse load performance between the floor and wall shocks in the 2nd TTI/SEM test series (#7 - #9). At first it was thought that the notable difference in the seatback's displacement between the driver's side (bottom) and passenger side (top) in the 2nd photo (Fig. 19.2) might help explain the difference in floor shock behavior, which was experienced in the 2nd test series but the wall and floor shocks' load histories are actually quite uniform (Figs. 24.5 & 24.6) and neither of the load histories are interrupted by any notable decreases. Also while the driver's side test dummy (bottom) had a faster spring back velocity (Fig. 19.4), than the other test dummies, due to the seatback's higher elastic deflection (Fig. 19.2) on the driver's side; all of the test dummies departed from the forward seat at about the same time (Fig. 19.3), which helps explain why the load history of the floor and wall shock zeroed at about the same time of 0.45 seconds (Figs. 24.5 & 24.6). As a side note it is believed that the reason for the difference in seat back deflections is probably due to the additional arm rest structure on the passenger's side (top) of the seat. Since the weight of the test dummies were about the same, there was no appreciable offset load to cause this difference in deflection. Lastly, if a close inspection of the four photos is made, one will note that there was very little travel of the seat's lower framework, which is the structure that the seat cushions rest upon. This can be seen by the lack of travel of the lower seat cushion, as well as the tips of the SEM shocks (tips are labeled in Fig. 19.1) remaining visible throughout the crash event (Figs. 24.1 - 24.4). So essentially the lower seat structures did not move relative to the floor attachments.

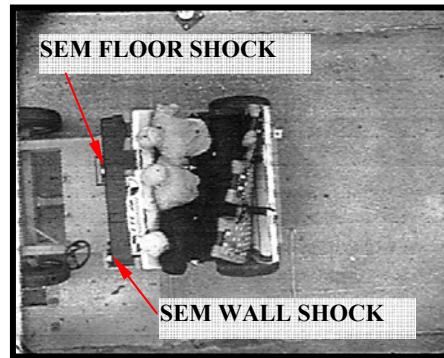


Fig. 19.1

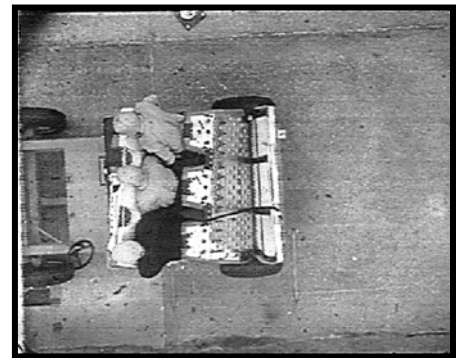


Fig. 19.2

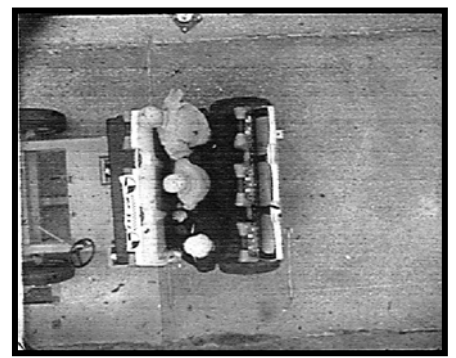
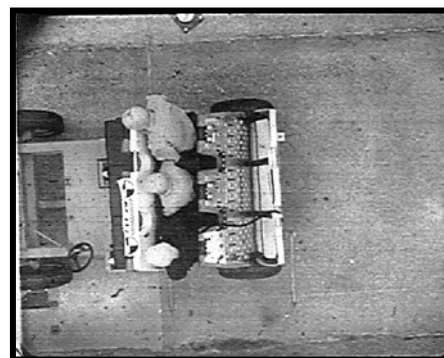


Fig. 19.4

19.3), which helps explain why the load history of the floor and wall shock zeroed at about the same time of 0.45 seconds (Figs. 24.5 & 24.6). As a side note it is believed that the reason for the difference in seat back deflections is probably due to the additional arm rest structure on the passenger's side (top) of the seat. Since the weight of the test dummies were about the same, there was no appreciable offset load to cause this difference in deflection. Lastly, if a close inspection of the four photos is made, one will note that there was very little travel of the seat's lower framework, which is the structure that the seat cushions rest upon. This can be seen by the lack of travel of the lower seat cushion, as well as the tips of the SEM shocks (tips are labeled in Fig. 19.1) remaining visible throughout the crash event (Figs. 24.1 - 24.4). So essentially the lower seat structures did not move relative to the floor attachments.

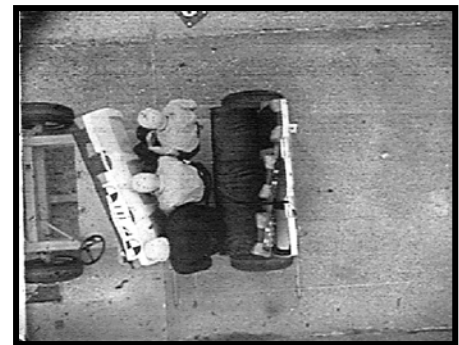


Fig. 19.5

While the forward seat in the 4th and 6th tests had some very similar crash loading and yielding behavior, some very valuable data also came from the 5th test, even though the bolt attachment for the floor shocks broke free (Fig. 19.5). If the seat shock load histories are reviewed for the 5th test (Figs. 24.3 & 24.4), there is the understandable drop off in load history for the floor shock's load cell (Fig. 24.4), since it broke free. The wall shock loading maintained a relatively constant load pulse, except for a brief load drop off possibly due to the seat swinging free from the Bogie vehicle's structures as well as momentarily losing contact with the test dummies. After that drop off, the loading then built back again to a slightly reduced pulse load. The dynamics of both seat test models (e.g. seats remaining attached or breaking free) are different, since the seat mass alone is the primary load mechanism in the 5th test series (e.g. no sustained test dummy loading) and the seat's two attach points where reduced to one attach point. This gives another example of how the wall shock loading can be relatively constant while the floor shock and/or the floor shock attach point goes through a more complex load history.

Unfortunately there were no overhead shots taken in the last three tests (#7 - #9) so there are no top views showing the forward seat dynamics with operable SEM seat shocks. Although, by considering the previously discussed seat dynamics from the first test series (#4 - #6) and employing the load and displacement data from the last three tests; a reasonable theory as to why the floor shock experienced a double pulse load can be postulated.

One of the ways the wall shock could experience a sustained load pulse while the floor shock experience a double pulse load (Figs. 24.8, 24.10, 24.12) would be if the forward seat had a similar rotation, but not as severe, as the breakaway rotation in the 5th test (Fig.

19.5). While again, there were no overhead shots to prove this behavior, the data appear to support the following scenario. When the test dummies' knees impacted the forward seat, the floor shock moved ahead at a faster rate than the wall shock, to where it absorbed much of the knee impact energy near the passenger side (top, Fig. 19.5, note the top dummy's knees are apparently no longer touching the forward seat structure). This movement continues at a faster rate on the passenger side until most of the momentum is transferred from the dummies' knees, on that side and the floor shock slows or stops momentarily relative to the Bogie floor. Since the wall shock was moving at a slower pace, it was still being loaded by the test dummy knees on the driver's side (bottom, Fig. 19.5). The second pulse on the floor shock occurred when the dummies' upper torsos and heads started hitting the seat back. The following test data appears to support such a scenario.

First, the floor shock traveled further than the wall shock in the 7th & 8th test (Table 5), whereas in the 9th test, both the seat and wall shocks traveled about the same maximum travel distance, since they used the softest durometer SEM and so the seat shocks in the 9th test just about bottomed out. To support the higher speed or rate of travel for the floor shock in the 7th & 8th test, note both seat shock types had almost identical pulse times, which initiated at about 0.11 sec and ended at about 0.45 sec (Figs. 24.7 – 24.10), so if the floor shocks moved further in the same time, they obviously were moving faster. Another piece of data that supports a similar but not as severe a seat rotation as shown in Fig. 19.5 comes from the femur load data (pg. 31). If the left and right femur load data is compared in the 4th and 6th test (Figs. 23.1 & 23.2, 23.5 & 23.6) there does not appear to be any distinctive difference between the left or right femur load histories, where one side was loaded with a greater or more sustained load pulse. Although, if the femur load histories are compared in the last three tests (Figs. 23.7 – 23.12) there is a distinctive difference in load pulse area (e.g. time or duration of pulse x-axis; size of pulse load y-axis) between the left and right femur load histories. Note that all of the g-load plots for the left femur (Figs. 23.7, 23.9, 23.11) are of greater area and therefore severity, than their right femur load counter parts (Figs. 23.8, 23.10, 23.12). This means the seat rotated enough, as in Fig. 19.5, to where the center test dummy's left femur experienced a more aggressive load history than the right femur. This point is supported from the similar femur load behavior that was experienced in the 5th test (Figs. 23.3 & 23.4), where the left femur load history is greater than the right femur load history.

Finally, a more detailed review of the raw accelerometer data, which was used to calculate the HIC performance numbers, was needed to determine when the center test dummy's head, which was the only one instrumented, was first making contact with the seat back (Figs. 22.1 – 22.18). Note: The HIC values were calculated on a neutral timeline since the actual contact timing of the test dummy's head was not needed to determine the HIC values. The most distinctive double load pulse was experienced in the 7th test run (Fig. 24.8) and the initiation of that second load pulse occurred at about 0.32 sec. If one now reviews the head accelerometer readings for the 7th test run (Figs. 22.10 – 22.12) there is a high, yet brief, initial spike load of about 135-g's at about 0.27 sec in Fig. 22.10. This spike load is probably due to the dummy's nose or lower jaw making initial contact with the seat back. At about 0.31 sec all of accelerometer readings for the dummy's head started to initiate, with relatively high and sustained g-loading (e.g. +25-g's in Fig. 22.10, -30-g's in Fig. 22.11, -40-g's in Fig. 22.12) and as it turns out this is about the same time the second load spike started to build in the floor shock's horizontal load cell (Fig. 24.8). This appears to support the theory that the seat rotated enough, as in Fig. 19.5, from the initial contact of the dummies' knees, then momentarily stopped relative to the floor shock and its x-axis load cell and then experienced a secondary pulse load from the collision of the dummies' upper torsos.

While the 8th test run did not have as a distinctive a load dip (Fig. 24.10) as the 7th test run, it still also experienced a dual spike load at about 0.35 sec, while the center dummy's head starting making substantial load contact at about 0.29 sec (Figs. 22.13 -22.15). The reason there was earlier head contact in the 8th test was due to the lesser travel of both SEM seat shocks (Table 5) as compared to the seat shock travel in the 7th test. This decreased travel time may help to explain why there was not as large a load dip. The dynamics of the 8th test varied from the 7th test in that the seat did not move forward as much as in the 7th test, so that there was more overlap of femur loading time and head contact times. This means just as the femur loading hit its 2nd minimum load at about 0.31 sec (Fig. 23.9), the center dummy's head had already started to load the seat back with its head at about 0.29 sec (Figs. 22.13-22.15); thus it's assumed the 2nd load pulse for the floor shock in the 8th test never went to zero, as in the 7th test run because of the greater overlap of the femur and head loading.

As to the 9th test run, it did not have as distinctive a load dip as the 7th & 8th test run. There was a minor load dip at about 0.26 sec (Fig. 24.12) which apparently was related to the secondary head impact loading since some of the large head accelerations occurred at about the same contact time, i.e., 0.27 sec (Figs. 22.17 & 22.18) but these performance loads were overwhelmed by the final peak loading experienced when both the wall and floor shocks bottomed out, at about 0.34 sec for the wall shock (Fig. 24.11) and about 0.30 sec for the floor shock (Fig. 24.12).

It should be noted that the raw 3-axis accelerometer data for the test dummy's head (Figs. 22.1 – 22.18) was added to this report to aid in the examination of the double pulse loading. There were some other performance parameters that were ascertained from the raw accelerometer data that were not apparent in the HIC performance plots. For instance, while all of the HIC performance plots had a wide range of deceleration behavior, to where none of the HIC plots were a close match, the plots still appeared to be relatively continuous, without any sharp and/or broken load spikes, except for the consistent initial load spike. While all of the x-axis or initial spike load plots from all of the tests (Figs. 22.1, 22.4, 22.7, 22.10, 22.13, 22.16) are relatively consistent, the remaining y-axis and z-axis accelerometer readings are quite telling.

For instance the remaining two accelerometer readings for the 4th test run (Figs. 22.2 – 22.3), both had a distinctive series of spike loads which is representative of structures or surfaces undergoing buckling or crushing. Since the 4th test had no displacement of the SEM seat shocks, this spike loading shows that the seat back was probably working to its design failure loads. Again, the 5th test run head accelerometer readings really were pertinent since the seat failed.

The 6th test run had some of the most distinctive load history even when using the raw accelerometer data. The highest load readings (Figs. 22.8 – 22.9) came near the end of the crash pulse loading unlike any of the other load histories, where the higher load pulses were near the beginning of the initial impact event (Figs. 22.2, 22.3, 22.11, 22.12, 22.14, 22.15, 22.17, 22.18). Plus, from this load

performance came the highest HIC values of all of the six test runs. At first it was thought that minimal displacement of the floor shock (e.g. final displacement 0.5") had little influence over the crash load performance. But, this may not be the case. There could be the possibility that the minimal deflection of the floor shock was just enough to prevent the seat back's failure loads from being achieved; so even if the loading was high, it was not enough to fail the seat back surface, which is needed to lower the HIC values. Also, there was very little displacement of the floor shock to provide an alternative means of energy absorption; thus instead of the HIC values being minimized, they were probably maximized with this minimal floor shock performance.

While not identical, the remaining accelerometer performances for the 7th – 9th test runs (Figs. 22.11, 22.12, 22.14, 22.15, 22.17, and 22.18) were actually quite close in their general performance. There were no abrupt load spikes as in the 4th test run (Figs. 22.2 -22.3) even though in the 8th test, it is known that the seat back did have a notable crush failure, which thereby reduced its HIC value. It is assumed that the rough load spikes of a seat back undergoing crush failure can be smoothed out with the additive deceleration behavior of the SEM seat shocks. While the SEM seat shock mods were not necessarily ideal for the seat model tested, the test data from the head accelerations does show the general crash load performances may be more repeatable than a surface undergoing buckling. So the possibility of adding a padded upper surface to the seat back's head contact zone, and the addition of some form of SEM seat shock mods may still be advantageous.



Fig. 20.1 TEST RUN 4



Fig. 20.2 TEST RUN 5



Fig. 20.3 TEST RUN 6



Fig. 20.4 TEST RUN 7



Fig. 20.5 TEST RUN 8



Fig. 20.6 TEST RUN 9

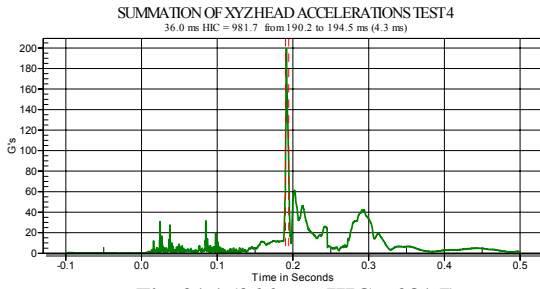


Fig. 21.1 (36.0 ms, HIC – 981.7)

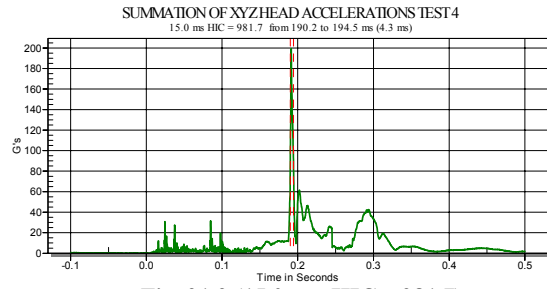


Fig. 21.2 (15.0 ms, HIC – 981.7)

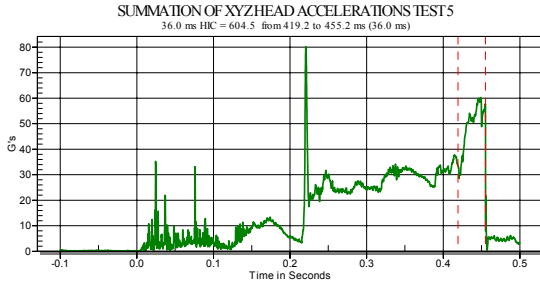


Fig. 21.3 (36.0 ms, HIC – 604.5)

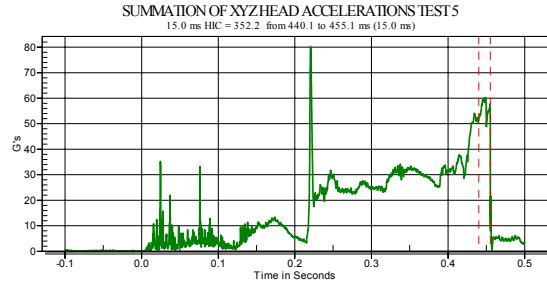


Fig. 21.4 (15.0 ms, HIC – 352.2)

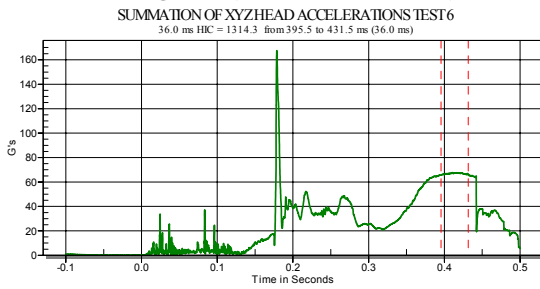


Fig. 21.5 (36.0 ms, HIC – 1314.3)

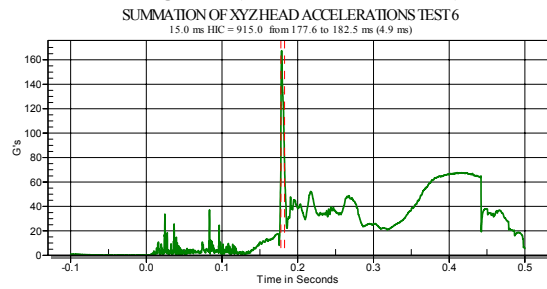


Fig. 21.6 (15.0 ms, HIC – 915.0)

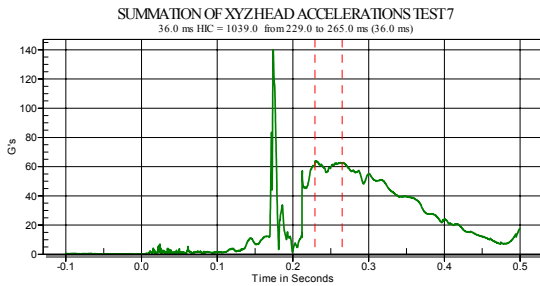


Fig. 21.7 (36.0 ms, HIC – 1039.0)

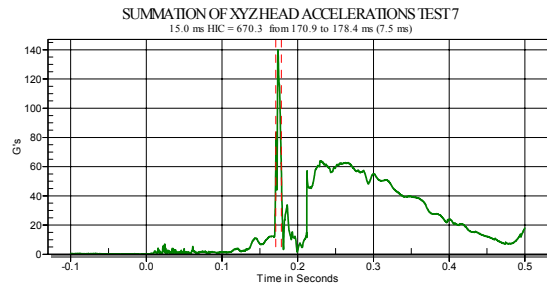


Fig. 21.8 (15.0 ms, HIC – 670.3)

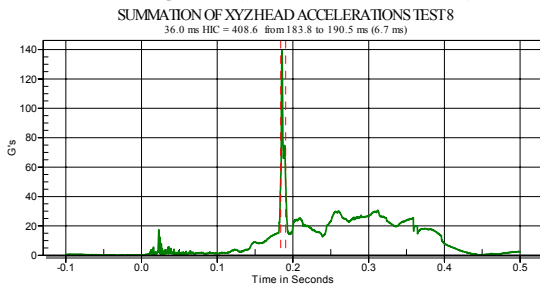


Fig. 21.9 (36.0 ms, HIC – 408.6)

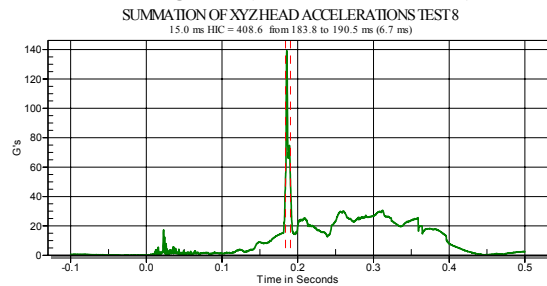


Fig. 21.10 (15.0 ms, HIC – 408.6)

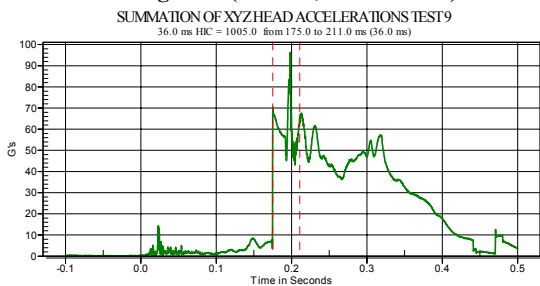


Fig. 21.11 (36.0 ms, HIC – 1005.0)

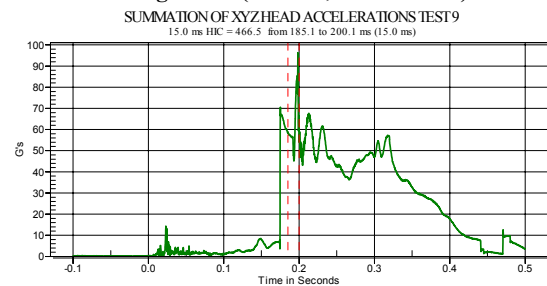


Fig. 21.12 (15.0 ms, HIC – 466.5)

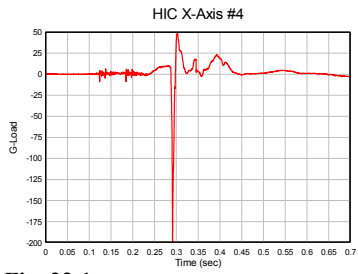


Fig. 22.1

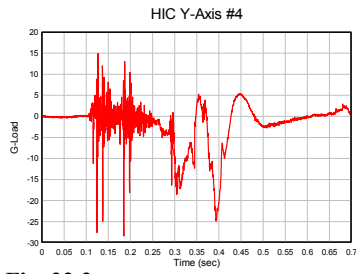


Fig. 22.2

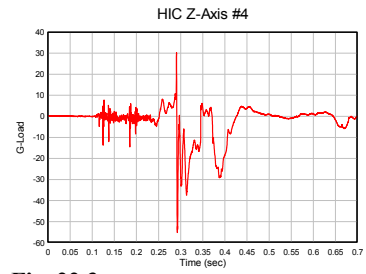


Fig. 22.3

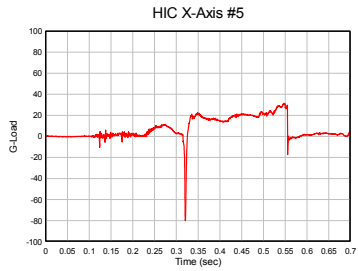


Fig. 22.4

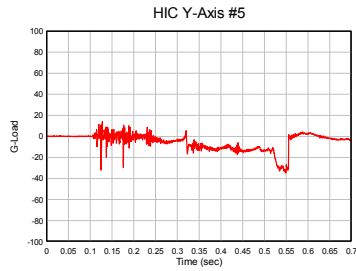


Fig. 22.5

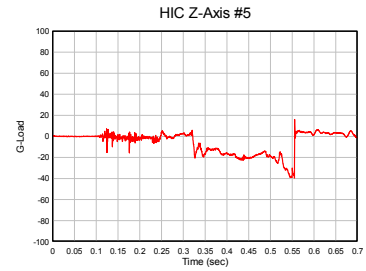


Fig. 22.6

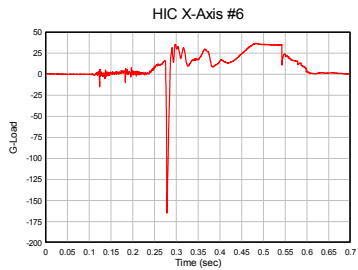


Fig. 22.7

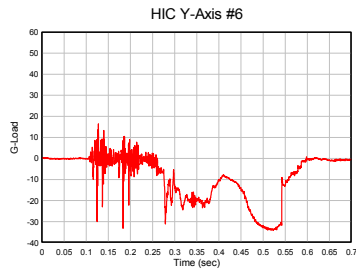


Fig. 22.8

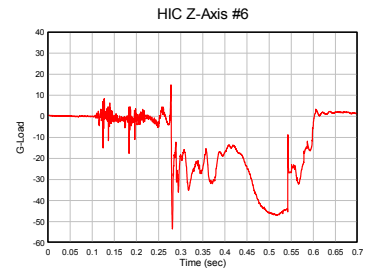


Fig. 22.9

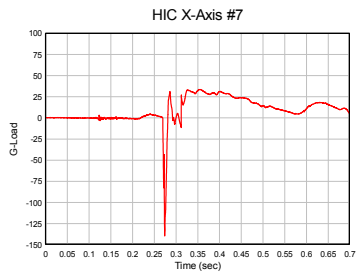


Fig. 22.10

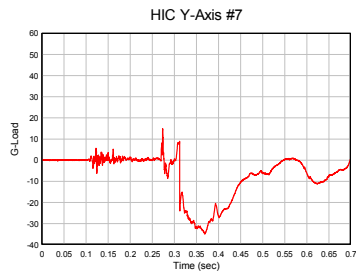


Fig. 22.11

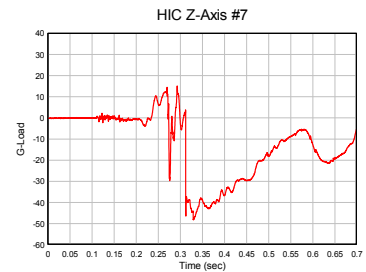


Fig. 22.12

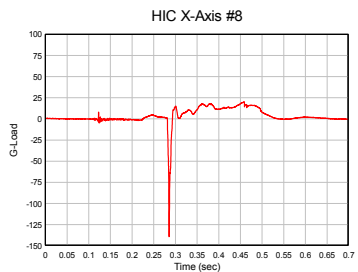


Fig. 22.13

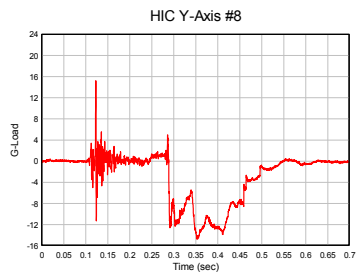


Fig. 22.14

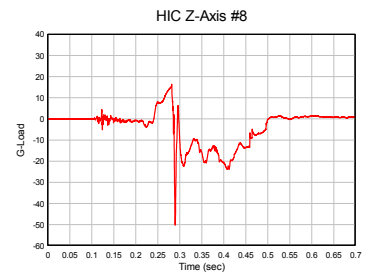


Fig. 22.15

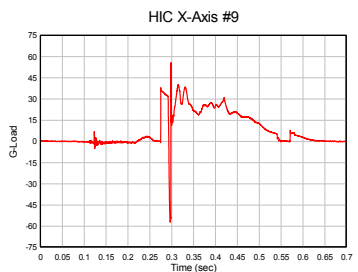


Fig. 22.16

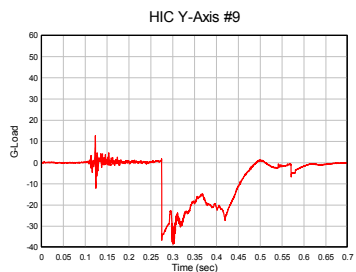


Fig. 22.17

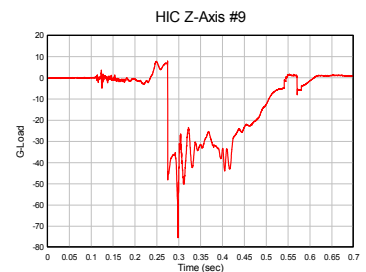


Fig. 22.18

Fig. 23.1

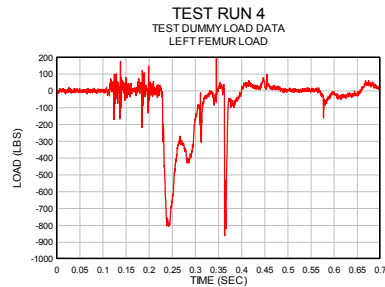


Fig. 23.2

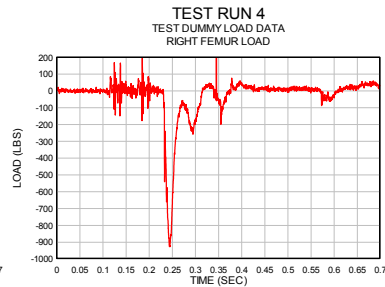


Fig. 23.3

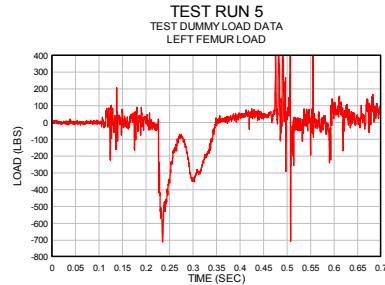


Fig. 23.4

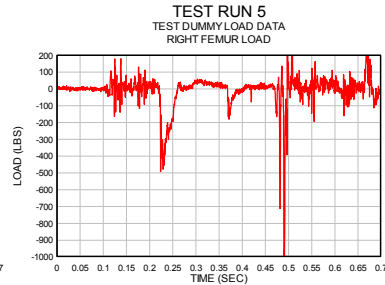


Fig. 23.5

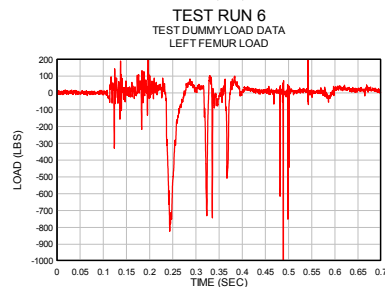


Fig. 23.6

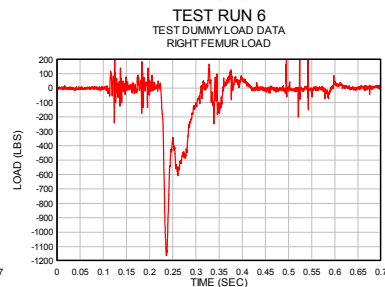


Fig. 23.7

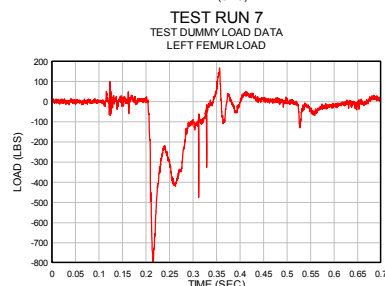


Fig. 23.8

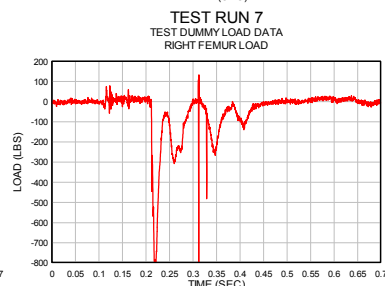


Fig. 23.9

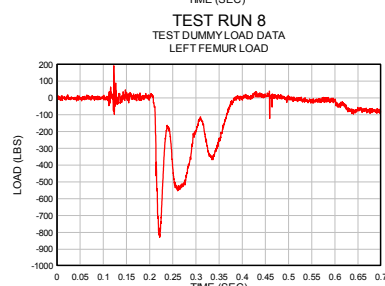


Fig. 23.10

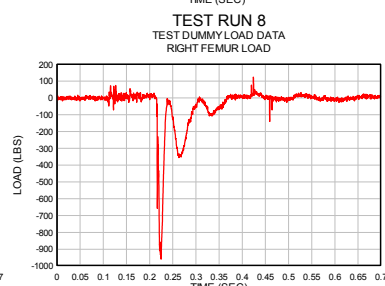


Fig. 23.11

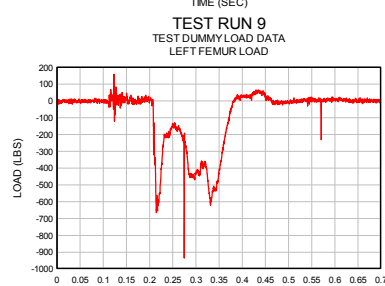


Fig. 23.12

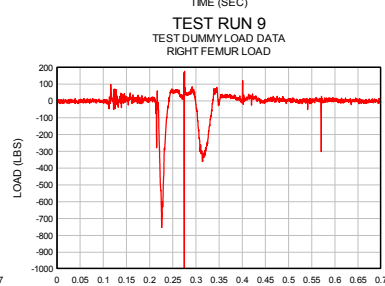


Fig. 24.1

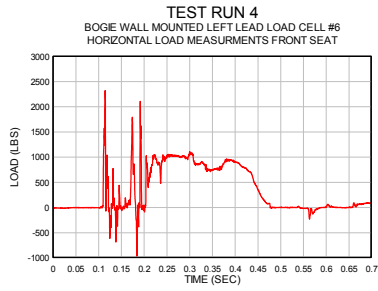


Fig. 24.2

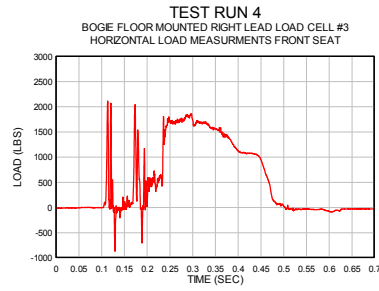


Fig. 24.3

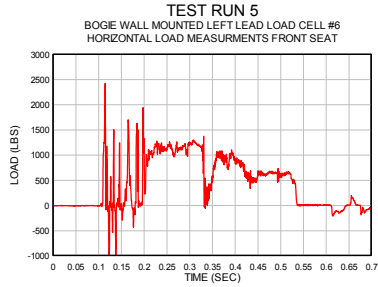


Fig. 24.4

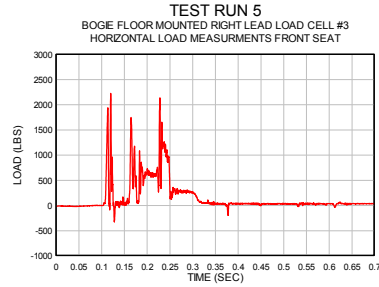


Fig. 24.5

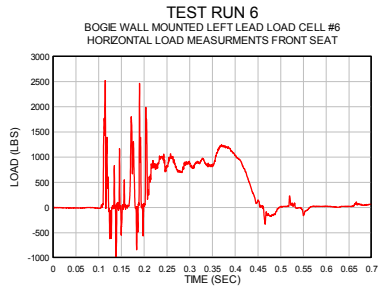


Fig. 24.6

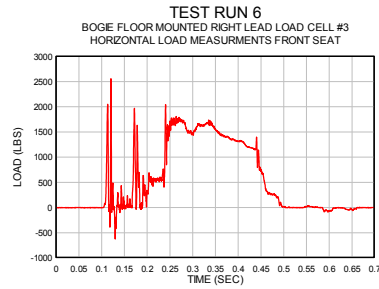


Fig. 24.7

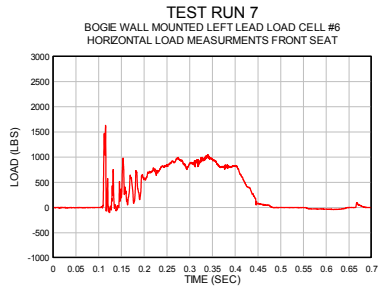


Fig. 24.8

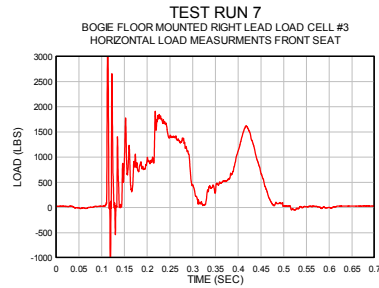


Fig. 24.9

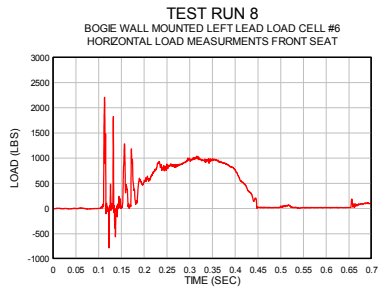


Fig. 24.10

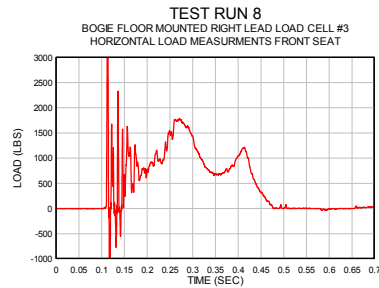


Fig. 24.11

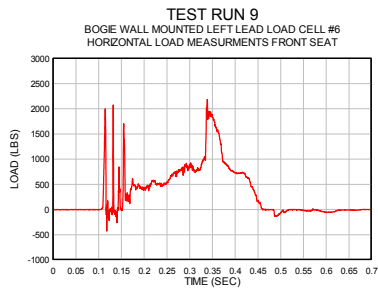
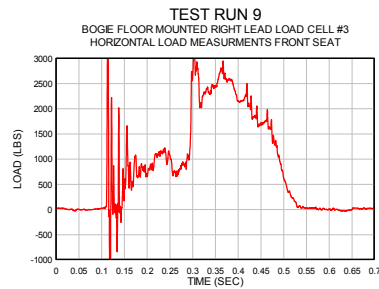


Fig. 24.12



CONCLUSIONS:

Comparison of head impact and femur load values with and without the SEM shocks revealed no significant differences in injury levels. Thus, the use of SEM technology for this specific application did not achieve the desired results. The reason the SEM seat shocks didn't provide a marked improvement in head and femur load values was essentially due to the initial impact environment (i.e., dummy's first contact with the seatback in the first 5 – 7 milliseconds) remaining about the same in seat tests with and without SEM shocks. The reason the test dummy experienced about the same initial contact loads was due to the relatively high inertia or mass of the seat (approx. 140 lbs.). Thus the dummy's initial contact with the fiberglass seatback was close to being unaltered between a stock and shock modified seat. To reduce the head-impact loads, the fiberglass seatback itself would need to be more like an airbag, i.e., it needs to be soft and/or yielding enough to reduce those initial load spikes. By making a softer surface the initial load spikes would be reduced, but it should be noted that while the majority of the peak head impacts measured by the instrumented dummies occurred in the initial load spike, some peak impacts occurred after the initial load spike. Therefore these remaining loads, after the initial load spikes, could be controlled by the yielding of the seat structures and/or displacement of the SEM seat shocks, thereby possibly reducing the later g-load history and kicking the peak impacts back to the region of the initial load spike. Thus, a notable improvement in the seat's head and femur load performances could be obtained if some type of soft/yielding seatback, especially near the top of the seat back, could be added to the seat design. Such a seat back change could maintain the seat's current steel framework, while probably not requiring an SEM seat shock modification.

A significant finding of this research was that the SEM shocks used in both the seat attachments and the impact barrier performed in accordance with the design specifications. Therefore, other applications of this technology are now being considered. There are other seat applications that experience a completely different type of load history than rail passenger seats, i.e., severe upward shock loadings. Examples are personnel seating in military vehicles that suffer mine blast loading and helicopter seats that experience severe vertical shock loads during emergency landings. The passenger in this type of seat shock environment will not suffer any of the previously-discussed spike loads, due primarily to the absence of free-flight travel. Passengers in these vehicles remain seated and in contact with the seat surface throughout the crash event. The SEM technology is an ideal method for reducing these high vertical load spikes and there is test history proving this point. Drop testing conducted at the Naval Undersea Warfare Center in 1996 duplicated such crash events in that a mass being supported by an SEM shock was dropped from a height of 5.5 ft thereby obtaining an impact velocity of 12.8 mph. Analysis of the data revealed no dramatic initial load spikes. The mass not protected by an SEM shock experienced a nearly 45-g deceleration but the impact piston, being supported by an SEM shock, only got up to a 13.7-g deceleration.

Plans for Implementation:

Present plans for implementation are limited. There are potential military applications such as improved vertical load seat shocks for military vehicles to reduce blast loading delivered to personnel by Improvised Explosive Devices (IEDs); and helicopter seats to provide more controllable shock isolation to personnel involved in emergency landings. There is a paper that discusses the various seat shock designs that are currently being used in helicopter seats (17). All of these systems use metal bending or shearing as the restraint mechanism. One of the drawbacks to the current designs is the lack of variable load control throughout a shock system's displacement. This desired performance feature could be obtained by employing the SEM technology. Currently, one large military vehicle manufacture is reviewing the SEM technology for mine blast seat shocks and other possible applications (e.g. vehicle airdrop platform shocks). Also, several automobile manufacturers and auto parts suppliers have been contacted, as well as some insurance companies and related vehicle test labs, in an attempt to get these companies to employ the SEM technology in vehicle bumpers to reduce the damage costs experienced in low- to moderate-speed impacts. A recent Insurance Institute for Highway Safety report (18) tested 17 new car models in a series of low-speed collisions. The resulting damages from these low speed impact tests were quite sizeable for most of the models tested. Three car models experienced over \$4,500 in damages in one 6 mph frontal collision. One of the past SEM test efforts was a series of seven impact tests using a full-sized 1989 Chevy pickup truck equipped with SEM bumper shocks (14). Impact tests were run on that Chevy pickup with speeds that varied from 3.5 mph up to 7.5 mph. No damage was delivered to the Chevy test truck other than the replacement or rework costs of the SEM bumper shocks. As to other SEM applications, there has been interest in landing shocks for NASA landing vehicles to replace current airbag systems. And lastly, when the needed funds become available, an Oregon company would be interested in representing a line of SEM Bumping Posts, which are used at the end of rail lines to keep railcars from going off the tracks.

References:

- 1). VanIngen-Dunn, C., March 2000, "Single Passenger Rail Car Impact Test Volume II: Summary of Occupant Protection Program", U.S. Department of Transportation, Federal Railroad Administration. http://www.fra.dot.gov/downloads/Research/ord0002_2.pdf
- 2). APTA SS-C&S-016-99, March 17, 1999, "Standard for Seating in Commuter Rail Cars", American Public Transit Association.
- 3). Tyrell, D.C., Severson, K.J., Marquis, B.P., 1995, "Analysis of Occupant Protection Strategies in Train Collisions", U.S. Department of Transportation. <http://www.fra.dot.gov/downloads/Research/asmeint2.pdf>
- 4). RAC, Revised November 8, 2001, "Railway Passenger Car Inspection and Safety Rules", The Railway Association of Canada, <http://www.railcan.ca/documents/RAIL-PASS-insp-01.pdf>
- 5). David Tyrell, Kristine Severson, A. Benjamin Perlman, March 2000, "Single Passenger Rail Car Impact Test Volume I: Overview and Selected Results", U.S. Department of Transportation, Research and Special Programs Administration, John A. Volpe National Transportation Systems Center. http://www.fra.dot.gov/downloads/Research/ord0002_2.pdf ***
- 6). Severson, T.K., October 1996, "Crashworthiness Testing of Amtrak's Traditional Coach Seat", U.S. Department of Transportation, Federal Railroad Administration. http://www.volpe.dot.gov/sdd/docs/1996/rail_cw_1996_2.pdf
- 7). Federal Register, October 4, 2002 (Volume 67, Number 193), "Improved Seats in Air Carrier Transport Category Airplanes", <http://www.epa.gov/fedrgstr/EPA-IMPACT/2002/October/Day-04/i25051.htm>
- 8). Cherry, R., Warren, K., Chan, A., "Benefit Analysis for Aircraft 16-g Dynamic Seats", U.S. DOT/FAA, Civil Aviation Authority London, England, http://research.faa.gov/aar/tech/docs/techreport/00_13.pdf
- 9). Mikhail, A.G., Army SBIR 2002, A02-033, "Low-Cost, Mine-Blast-Resistant Crew Seat for Interim Armored Vehicle (IAV) and Future Combat System (FCS) Ground Vehicles of the Objective Force".
- 10). Status Report - Insurance Institute for Highway Safety, Special issue: Side impact crashworthiness; Vol. 38, No. 7, June 28, 2003, <http://www.highwaysafety.org>
- 11). Footnote: While the table is not clearly labeled in reference (3) as an "HIC_{BB36ms}" value, the only HIC value that was accepted at the time reference (3) was written, and that was the HIC_{BB36ms} = 1,000. Subsequently, NHTSA has introduced the HIC_{15ms}, thus the original HIC is now represented as HIC_{BB36ms}.
- 12). Kenneth G. Budinski, "Engineering Materials Properties and Selection", pg. 158, Prentice-Hall, Inc., New Jersey, 1996.
- 13). Stephen E. Knotts, Vehicle, 01IBECD-2, 2001 Society of Automotive Engineers, Inc., "Crash Performance Augmentation Through SEM (Solid Ejection Material) Shock Isolation"
- 14). VanIngen-Dunn, C., Manning, J., "Commuter Rail Seat Testing and Analysis," US Department of Transportation, DOT/FRA/ORD-01/06, July 2002, http://www.volpe.dot.gov/sdd/docs/2002/rail_cw_2002_5.pdf
- 15). Rolf Eppinger, Emily Sun, Faris Bandak, Mark Haffner, Nopporn Khaewpong, Matt Maltese, HTBRC; Shashi Kuppa, Thuvan Nguyen, Erik Takhounts, Rabih Tannous, Anna Zhang, Conrad Technologies, Inc.; Roger Saul, VRTC; November 1999, "Development of Improved Injury Criteria for the Assessment of Advanced Automotive Restraint Systems – II", NHTSA, http://www-nrd.nhtsa.dot.gov/pdf/nrd-11/airbags/rev_criteria.pdf
- 16). Brian G. McHenry, "Head Injury Criterion and the ATB", ATB Users' Group 2004, <http://mchenrysoftware.com/HIC%20and%20the%20ATB.pdf>
- 17). Stanley P. Desjardins, "The Evolution of Energy Absorption Systems for Crashworthy Helicopter Seats", http://www.fire.tc.faa.gov/2004Conference/files/crash/S.Desjardins_Energy_absorption-helicopter_seats.pdf
- 18). Insurance Institute for Highway Safety, "New Crash Tests Show High Cost of Bumpers that Fail to Bump", Vol. 42, No. 2, March 1, 2007, <http://www.iihs.org/sr/pdfs/sr4202.pdf>

Glossary:

ATD – Anthropomorphic Test Device (or Dummy) – A device designed to look and respond like a human in a crash environment. ATDs are usually instrumented to measure such things as head impact, chest acceleration and axial femur load during a crash test. Different ATDs are used to represent different body types, e.g., 95th percentile male, 50th percentile male, 95th percentile female, children and infants. As an example, only 5% of the adult male population is larger and heavier than the 95 percentile male ATD.

Durometer – D – Is normally a measure of the hardness of a plastic or rubber (polymer) but it can also be a measure of a polymer’s shear and/or flow characteristics. The Durometer A hardness measure was the method used to classify the rubber compounds used in the HSR-45 study. The range of Durometer A values normally vary from 30-D to 90-D (Note: some lower durometer values can be made on special order) with the higher durometer values equating to harder materials. There are actual five different methods for measuring the hardness of a material (12), depending on the material type, those being; Brinell Hardness for metals (steel, copper); Rockwell M (Nylon) & Rockwell R (Polypropylene) for harder plastics; Durometer D for elastomers (Urethanes) and some plastics (Polyethylene); and Durometer A for only elastomers (Natural Rubber, Butyl Rubber).

HIC – Head Injury Criteria – Is a method to attempt to quantify the injury levels to a person’s head, during a vehicle collision, when that person’s head impacts some surface (e.g. seat back, airbag). The HIC formula has progressed over the years (15), from the Wayne State Tolerance Curve (WSTC) to the Gadd Severity Index GSI (1966), then to Versace’s initial version of the HIC in 1971 (See formula below). In the initial version of the HIC formula there were no set time intervals, instead t₁ would be an arbitrary start time and t₂ would be an arbitrary end time, a(t) is the resultant head acceleration and would be in units of g’s or acceleration of gravity and t

$$HIC = \left\{ (t_2 - t_1) \left[\frac{1}{(t_2 - t_1)} \int_{t_1}^{t_2} a(t) dt \right]^{2.5} \right\}_{\max}$$

would be in seconds. It should also be noted that the HIC formula took into account the resultant transitional acceleration (ax, ay, az) of all three axes, instead of just the frontal axis (ax) which was used in the original WSTC (16). In the October 17, 1986 Federal Register Notice, the NHTSA indicated that it had decided to limit the HIC time interval to 36 milliseconds (15), plus set an HIC value of 1000 for this time interval (HIC_{36ms}=1,000) for a 50th percentile male. Also, note that the HIC_{36ms} value taken from a particular crash pulse must be the maximum HIC_{36ms} value obtainable for that crash pulse. The next two points regarding a passenger’s head injury level should be considered when a railcar seat experiences the HIC_{36ms} = 1, 000 value, those being:

1. “The HIC is unique among FMVSS 208 injury criteria in that the HIC limit of 1000 was NOT based on tests where HIC was measured and injuries observed. The HIC has no specific meaning in terms of injury mechanism”. (16).
2. “AAMA also argued that HIC_{36ms} overestimates the risk of injury for long-duration head impacts with air bags. That organization cited a study where human volunteers who were restrained by air bags experienced HIC_{36ms} greater than 1000 and did not experience brain injury or skull fracture.” (15).

So it should be noted that while some of the HIC values measured in the HSR-45 study, did slightly exceed the HIC_{36ms}=1,000 spec value, this does not necessarily mean that severe injuries would have been experienced by actual railcar passengers.

A shorter duration HIC value had been considered for years but as of 2000(16) the NHTSA finally decided on the following HIC values over a 15 millisecond time interval (HIC_{15ms}) for a range of occupant sizes.

Table 1S1-1: Head Injury Criterion for Various Dummy Sizes

Dummy Type	Large Sized Male*	Mid-Sized Male	Small Sized Female	6-Year-Old Child	3-Year-Old Child	1-Year-Old Infant
HIC _{15ms} Limit	700	700	700	700	570	390
*The Large Male (95 th percentile Hybrid III) is not included in the final rule, but the performance limits are listed here for informational purposes						

It should be noted that both methods for calculating the HIC values (HIC_{36ms} & HIC_{15ms}) were run in the HSR-45 study and there was an interesting overlap in the pass-fail criteria between the 36ms and 15ms HIC values. Five out of six seat tests obtained valid HIC values (seat broke free in the 5th test run), where two of the test runs had HIC_{36ms} & HIC_{15ms} values that agreed (e.g. both HIC values failed in the 6th test and both of the HIC values passed in the 8th test); but in the remaining three tests the HIC values did not agree. The following table gives the two HIC values for the HSR-45 test.

Test Run #	HIC _{36ms} = 1,000	HIC _{15ms} = 700	Pass/Fail
4	981.7 / Pass	981.7 / Fail	Didn't Matched
5	Seat Detached	Seat Detached	N/A
6	1314.3 / Fail	915.0 / Fail	Matched
7	1039.0 / Fail	670.3 / Pass	Didn't Matched
8	408.6 / Pass	408.6 / Pass	Matched
9	1005.0 / Fail	466.5 / Pass	Didn't Matched

Note, that the HIC_{36ms} values in the 7th & 9th tests came very close to the 1,000 value, also note that all of the HIC_{15ms} in test runs 7th through 9th tests all came in below the spec 700 value, and these last three test runs did have SEM seat shocks that underwent substantial displacement.

At the time of the tests, the TTI test personnel and principle investigator had a question as to how there could be a pass/fail overlap in the HIC values, for the same tests, and while this pass/fail overlap was very high (60%) for the HSR-45 study, this overlap is not unusual. For instance, there have been past crash tests that has exhibited some level of this pass/fail overlap between the two HIC values. The NCAP ran 295 crash tests and “of the 295 NCAP tests examined, 260 passed and 18 failed both criteria, 10 tests that failed HIC₁₅ passed HIC₃₆, while 7 tests that failed HIC₃₆ passed HIC₁₅” (15).

SEM – Solid Ejection Material – This is a general term that is used to describe the flow medium for an SEM shock set, and that flow medium provides the back pressures needed to restrain the travel of the SEM shock piston. While there is a large list of materials that can fit into the classification of SEM type materials, not all solids can meet the needed flow and/or shear characteristics of an SEM type material. For instance, even though many of the materials used to date have been polymers (e.g. plastic & elastomers), some polymers would just not work, such as, many nylon compounds or the typical resin based fiberglass. Such materials have a brittle type of displacement or failure mode, where the material cracks and fails, much like a ceramic, glass or concrete solid. Some other materials, which have not been tested to date, also fall into the SEM classification those being some of the metal alloys. While many of the typical SEM shock parts are harden steel parts (e.g. piston & shock housing), some “softer” or more ductile metals could be employed as the Solid Ejection Material, such as, aluminum, lead, tin, copper. While there is some overlap of the ejection pressures between the harder polymers and softer metals (e.g. 30,000 – 40,000 psi range) most of the soft metals can supply pressure loads that are more than double that of the polymers max flow pressures. Some of these metallic flow mediums will be explored at some future date.